Further Correlation of Magnetic Profile Data with Basement Structure of the Bellefontaine Outlier, Ohio

A Senior Thesis

Submitted as Partial Fulfillment of the Requirements
For the Degree Bachelor of Science in
Geological Sciences at
The Ohio State University

by

Joshua D. Kozlowski

The Ohio State University

Spring 1998

Dr. Hallan C. Noltimier

Acknowledgements

This paper represents one of the many accomplishments to my name that I'm honestly very proud of. I would really like to extend my deepest thanks to my wonderful advisor, Dr. Noltimier. Without his guidance and encouragement, none of this would have happened. I would also like to thank Christian Steck for his input on some of my figures and diagrams. Kelley Kaltenbach's help was vitally important and cannot be overlooked. A special thanks goes to Brent Curtiss for help with aiding me in fixing computer problems. I would also like to thank my parents as well for all of their encouragement and much needed support. Lastly, I did not give up when the workload seemed insurmountable.

TABLE OF CONTENTS

LIST OF FIGURES

LIST OF TABLES

INTRODUCTION

Campbell Hill is the location of the highest point in the state of Ohio, and it attains a height of 1579 feet (482.9 m.) above sea level. However, it is also relatively unimpressive in that the hill only rises around 40 feet (12 meters) or so from the topography surrounding it. In fact, the hill probably wouldn't be noticeable if it weren't for the 80-foot (24 m.) thick covering of glacial till. However, this high point is notable in that it lays astride to the Devonian outcrop known as the Bellefontaine Outlier (Hansen, 1997).

The Bellefontaine Outlier is a completely isolated outcrop of Devonian age rocks. The nearest rocks of equivalent age lay 30 miles (48 km.) to the east. The isolation of this outcrop makes the area worth investigation. In 1992, John Weaver conducted a potential field study by taking magnetic readings at 510 different stations over an area of over 500 square miles (805 $km.^2$) (Weaver, 1992). The most recent interpretation is that the Outlier is the surface expression of a reverse half-graben or reverse full-graben structure.

The interpretations were made trying to take into account as many different types of data that were available. These data types include gravity and magnetic measurements (Weaver, 1992), the COCORP (Consortium for Continental Reflection Profiling) profile (Hansen, 1989), and the aeromagnetic map of Ohio (Lucius and Von Frese, 1988.) My

objective was to verify the most recent interpretation of the structure and to also try to refine the interpretation if possible. The attempt was to better understand the relationship between Precambrian crystalline basement structure with the surface expression of the Bellefontaine Outlier.

An introduction to the geology of the study area and surrounding region, including the Bellefontaine Outlier, is followed by a discussion of the magnetic profiles and their significance.

REGIONAL GEOLOGY

General Tectonic History

In Ohio, the oldest known geologic events happened about 1.4-1.5 Ga. before present. It was during this time that a seven-mile thick layered slab of granite and rhyolite was emplaced, probably due to a superswell, or an uprising in the Earth's mantle. This formed what we now refer to as the Granite-Rhyolite Province. This upwelling caused continued doming under western Ohio, Indiana, and Kentucky and led to the creation of a complex rift basin known as the East Continent Rift Basin (ECRB) though extensive faulting and down-dropping (Hansen, 1996). This basin is most likely a part of the Keweenawan Midcontinent Rift System. The Middle Run Formation now fills this basin. The thickness of this basin-fill unit is extremely variable and reaches a thickness of 20,000 feet (6000 m.) along the Grenville Front Boundary with a maximum mapped thickness of 22,500 ft. (Drahovzal et al, 1992). Roughly about 1 Ga. before present, the doming ceased which brought the rifting, volcanic activity, and basin filling to an end, resulting in a failed or aborted rift (Hansen, 1996). Figure 1 shows an interpretation of the sequence of events that caused the creation of the ECRB and the basement structure beneath the Bellefontaine Outlier.

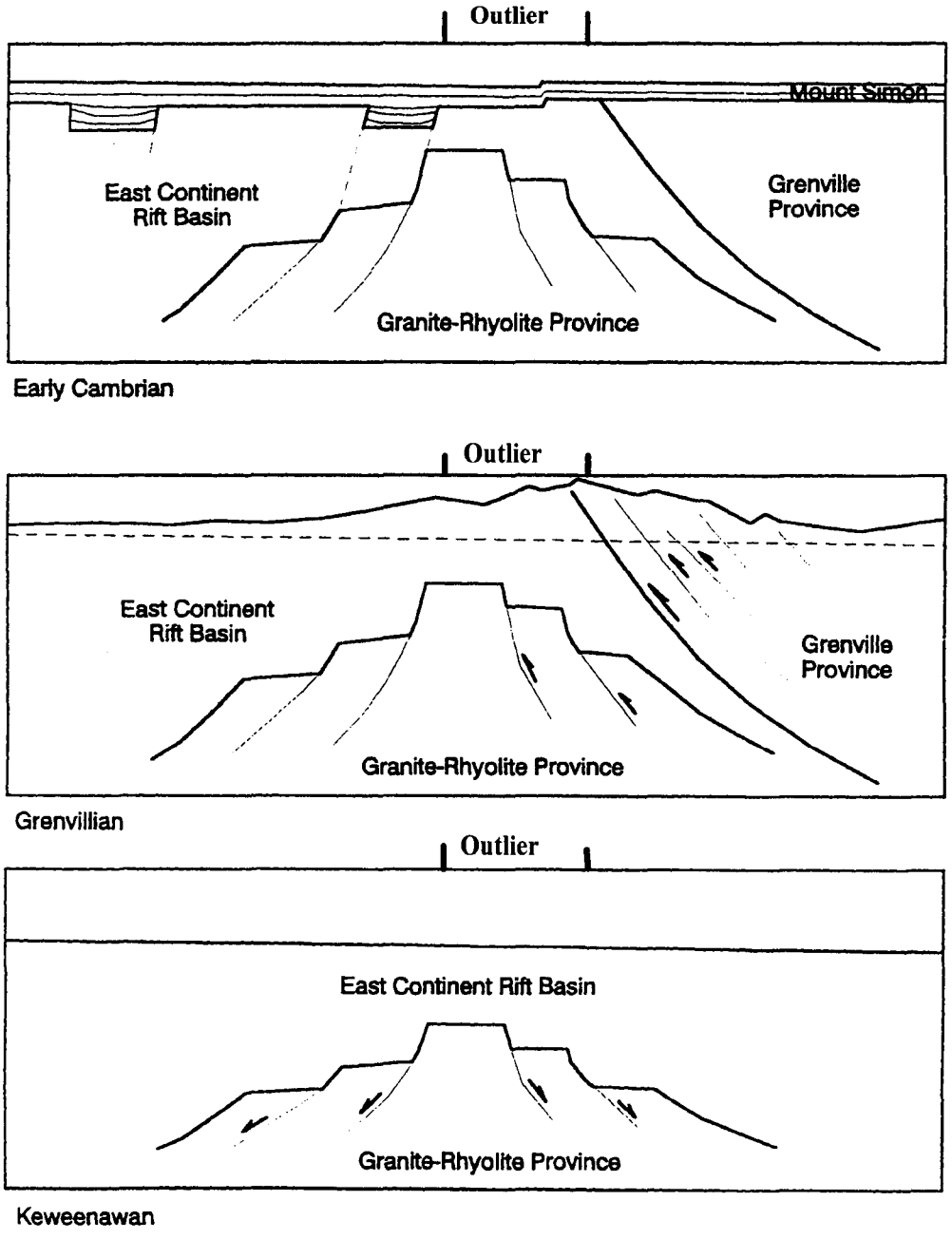

Figure 1 – Interpretation of how the ECRB was formed from the Precambrian through the Early Cambrian, modified from Steck et al, (1997).

The Grenville Mountains were created between 990-880 Ma. through a continental collision on the eastern side of North America, during the Grenville Orogeny (figure 2). The Grenville Mountains stretch 3000 mi. (4800 km.) down from Northern Canada. The suture zone of the two continents (that formed this mountain chain) was discovered though the COCORP profile (1987) in Coshocton County. This suture zone is aptly named the Coshocton Zone (Hansen, 1996). The Grenville Front Tectonic Zone is 30 miles wide and consists of east-dipping thrust slices and notes the westward trend of the Grenville Mountains (Hansen, 1996). The probable extent of the Grenville Mountains in Ohio is shown in Figure 3.

A 300 Ma period of deep erosion followed the formation of the Grenville Mountains. It was during this time period (Late Precambrian) that these mountains were eroded away and considerable cummulative lateral displacement by strike-slip faulting occurred (Hansen, 1996).

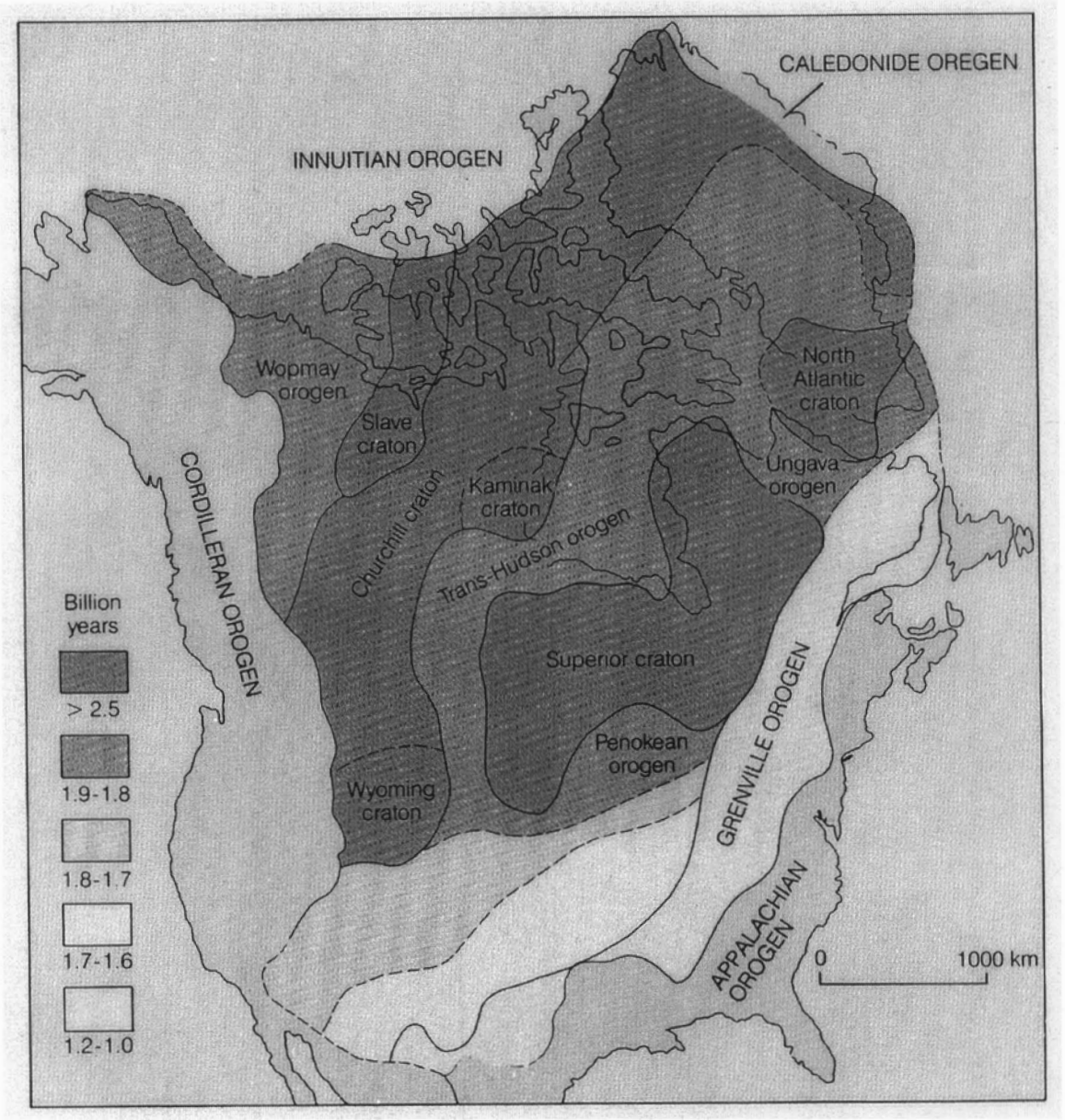

Figure 2 – Map showing the actual dates of orogenic Events in present day North America, modified from Hoffman, (1988).

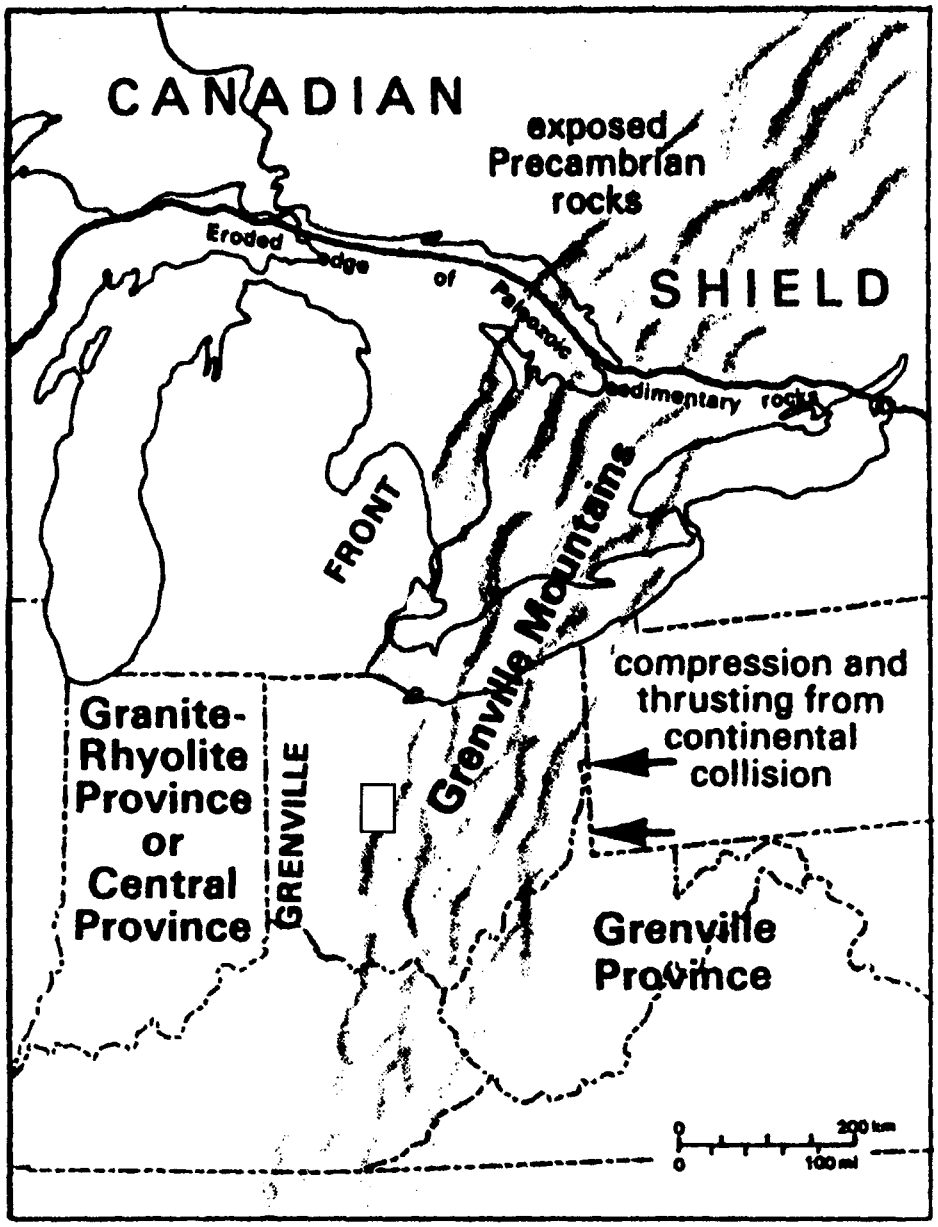

Figure 3 – Map showing the probable extent of the Grenville Mountains into present day Ohio, modified from Hoffman, (1988).

Precambrian Section

Precambrian Crystalline Basement

The only rocks from the Precambrian crystalline basement have come from the borehole samples, because these rocks do not crop out anywhere in the state. The nature of their structure can only be determined by geophysical methods. Geophysical data points to the fact that the Grenville Tectonic Front Zone is present above these basement rocks.

Granite-Rhyolite Province

The Granite-Rhyolite Province is a seven mile thick body of layered granites and rhyolites that were emplaced by an uprising in the earth's mantle around 1.4-1.5 billion years ago. The province is located beneath 5000-15,000 feet (1530-4600 meters) of the Middle Run Formation. In the study area, the province lies at a depth from -7500 to -15,000 ft. (-2300 to -4600 m.) (Wickstrom et al., 1992).

East Continental Rift Basin (ECRB)

The East Continental Rift Basin (ECRB) was formed during Late Proterozoic and is probably part of the Keweenawan Midcontinent Rift System. The thickness of the ECRB is maximum along and just to the west of the Grenville Front. Uplifting from regional compression caused

the ECRB to gradually thin towards the west, and the ECRB is filled by the Middle Run Formation (Wickstrom et al, 1992).

To the east of the ECRB is the Grenville Province. The boundary of these two is believed to lie beneath the Grenville Front. It is also thought that the ECRB and the Grenville Province is part of a complex wrench-fault system (Drahovzal et al, 1992).

Grenville Front Tectonic Zone

The Grenville Front Tectonic Zone (GFTZ) stretches 2500 miles (4000 km.) and represents the western edge of the Grenville Mountains (Hansen, 1989). It has also been altered by intense stresses from several different continental collisions. During the Grenville Orogeny (Late Proterozoic), compression from the mountain building events caused thrusting that was later modified by wrench faulting. The GFTZ borders the Grenville Province to the east and is adjacent to the ECRB to the west (Wickstrom et al, 1992).

Grenville Province

The Grenville province was formed between 880 and 990 million years ago. The Province is made up of mostly metamorphic rocks. The regionally metamorphosed igneous rocks of noting are granite-gneiss, schist, horfels, amphibolite, and marble (Lucius and Von Frese, 1988). The Grenville Province borders the ECRB to the east. The COCORP

profile not only identified the province, but it also allowed the discovery of the 100 mile wide feature area known as the Coshocton Zone (Steck, 1997). This zone was interpreted as the suture zone of the continents that formed the Grenville Province.

Precambrian Unconformity and Basement Structure

The crystalline basement rocks are separated from the overlying younger sedimentary rocks by an unconformity. After the Grenville mountains were formed, they were heavily eroded during a period of 300 million years, in the late Precambrian. This set of erosional events also is thought to have removed the top part of the ECRB (Steck, 1997).

Paleozoic Section

Paleozoic Sedimentary Rock Units

These Paleozoic sedimentary rock units are date from the Cambrian to the Permian in age. Most of these units consist of dolomites and shales. The deposition of these sediments was greatly influenced by reactivated older faults. Regional tectonics during the Acadian Orogeny is thought to be responsible for the reactivation of these faults.

BELLEFONTAINE OUTLIER

Introduction

The Bellefontaine Outlier is a body of north-south trending Devonian rocks, which occupies central Logan and northern Champaign Counties. The closest location of an outcrop of Devonian age rocks is roughly 30 miles (48 km.) to the east (figure 4). The Outlier was thought to be relatively higher than it's surroundings during the middle Devonian. This is evidenced by the absence of the Delaware Limestone and the Olentangy Shale. Two possibilities are that either the two units were never locally deposited or the units were eroded away after they were deposited. The Outlier is surrounded by older Silurian age dolomites.

Origin

The youngest bedrock of the Bellefontaine Outlier was formed during the Devonian (380 Ma) when the environment was much different in what we now call Ohio. A shallow, warm, subtropical sea covered most the state, and limy mud (that formed the Columbus Limestone) was deposited. In the late Devonian, the sea that covered the area was in places much deeper causing finer particles to settle out, forming the unit known as the Ohio Shale (Hansen, 1997).

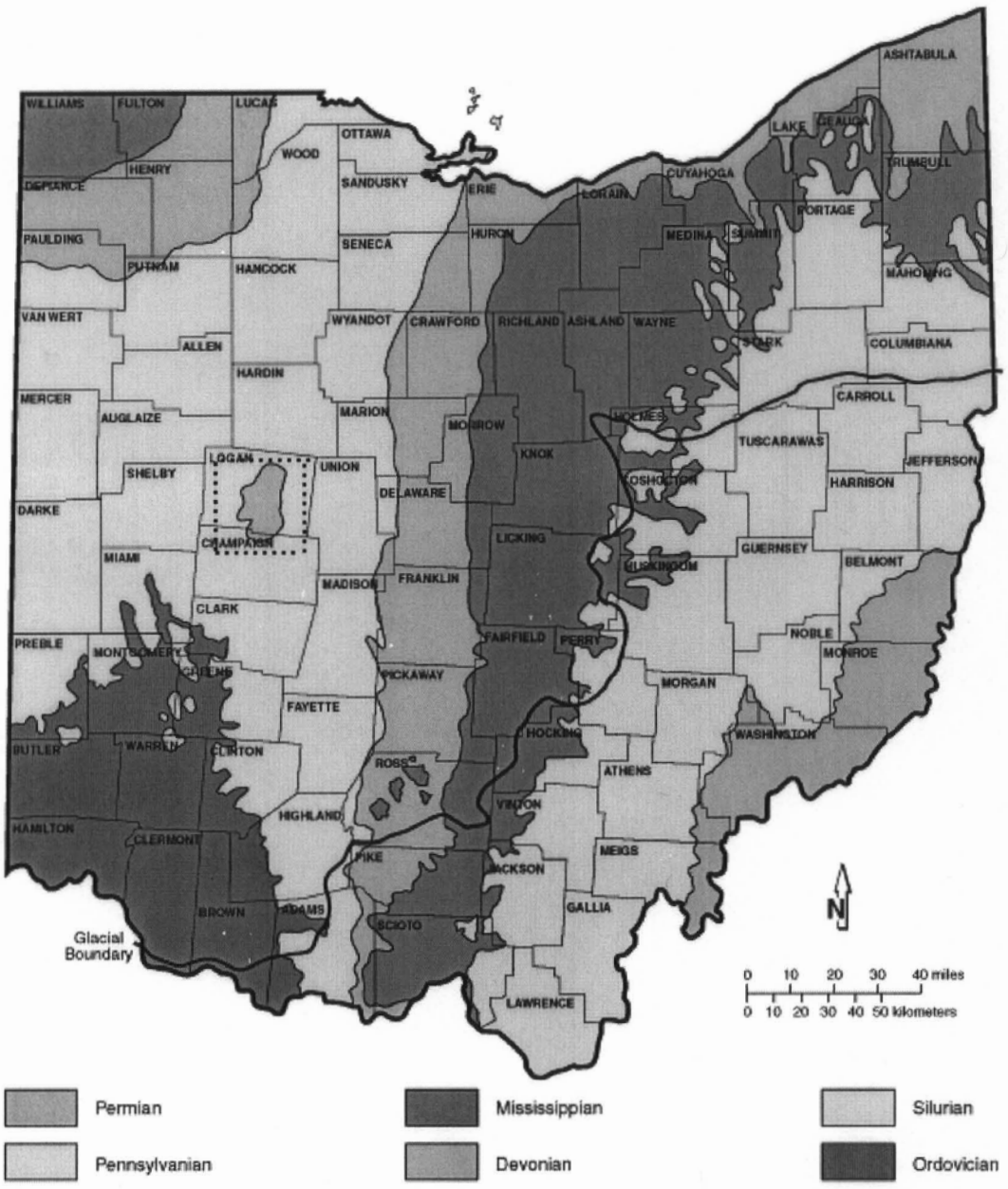

Figure 4 – Map showing the distribution of bedrock by their respective ages. Study area is noted by the dotted box, modified from Steck et al, (1997).

Stratigraphy

The study area consists of a stack of units that are Proterozoic, Paleozoic, and Quaternary in age. The units in the study area boundary are given in the stratigraphic column (figure 5). The Granite-Rhyolite Province underlies the Bellefontaine Outlier. The Paleozoic units age range between the Cambrian through the Devonian. Limestones, sandstones and dolomites primarily make up the Cambrian age rocks. Interbedded limestones and shales make up the Ordovician strata. The Silurian age rocks are argillaceous or shaly dolomites with some dolomitic shales and limestones. Dolomites and carbonaceous shales make up the Devonian units. The surface is covered with a varying thickness of Quaternary glacial drift.

Structure

The structure of the Bellefontaine Outlier was determined from the COCORP OH-1 Seismic Line in 1987. It has been interpreted as a reverse half-graben or reverse graben structure. High angle reverse faults surround an uplifted block (Steck, 1997). The Outlier is also presently located just west of the Grenville Front Tectonic Zone. The COCORP line shows east-dipping layered rocks over a footwall ramp of the Grenville Front. These Precambrian faults are believed to have influenced the stratigraphic history and structure of the overlying Phanerozoic sediments. (Wickstrom et al, 1992).

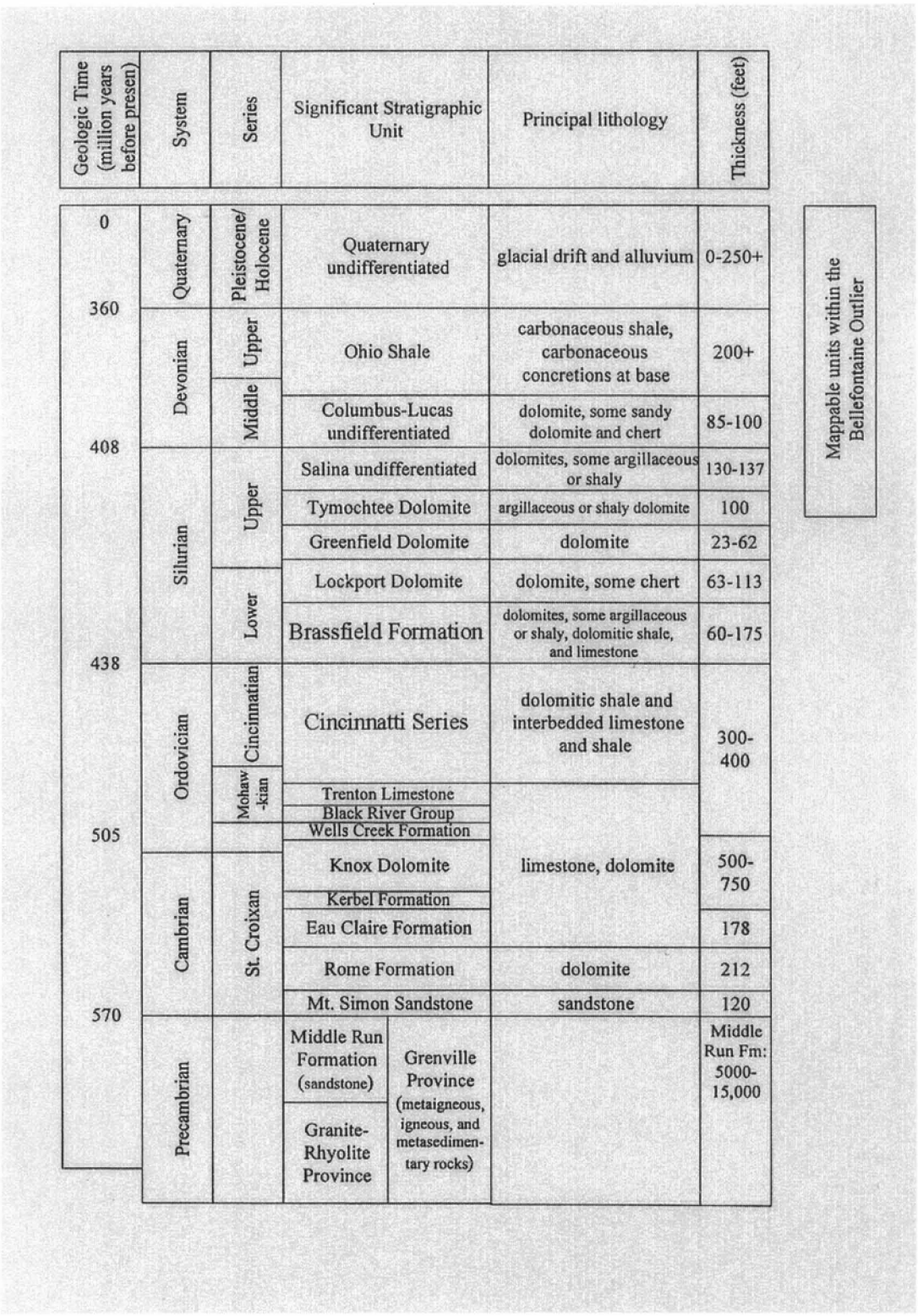

Figure 5 - Generalized stratigraphic column in Bellefontaine Outlier Survey Area. (Modified from Steck, 1997.)

MAGNETIC PROFILES

Introduction

Figure 6 shows the underlying structure of the study area. Changes were made to this interpretation by Steck's fault calculations (Figure 7). This data was gathered by Weaver (1992) and was responsible for the preliminary analysis of the study area.

The Magnetic Residual Anomaly data was gathered through an intense survey of the Bellefontaine Outlier Study Area (Weaver, 1992) by taking magnetic readings from 510 different stations (Figure 8). These were used to generate the 300 gamma filter magnetic residual anomaly map (Figure 9). This map was originally generated by Weaver (1992) and was reconstructed by the same methods that Weaver used. Figure 10 is essentially the same as figure 9 with the difference being that figure 10 illustrates the number and location of each of the profiles that were investigated as part of my study.

Methods

In order to interpret the structure and stratigraphy of the Bellefontaine Outlier, some basic assumptions were made. All of the faults within the study area boundary were assumed to be vertical or nearly vertical. This assumption was made in order to simplify the fault throw calculations.

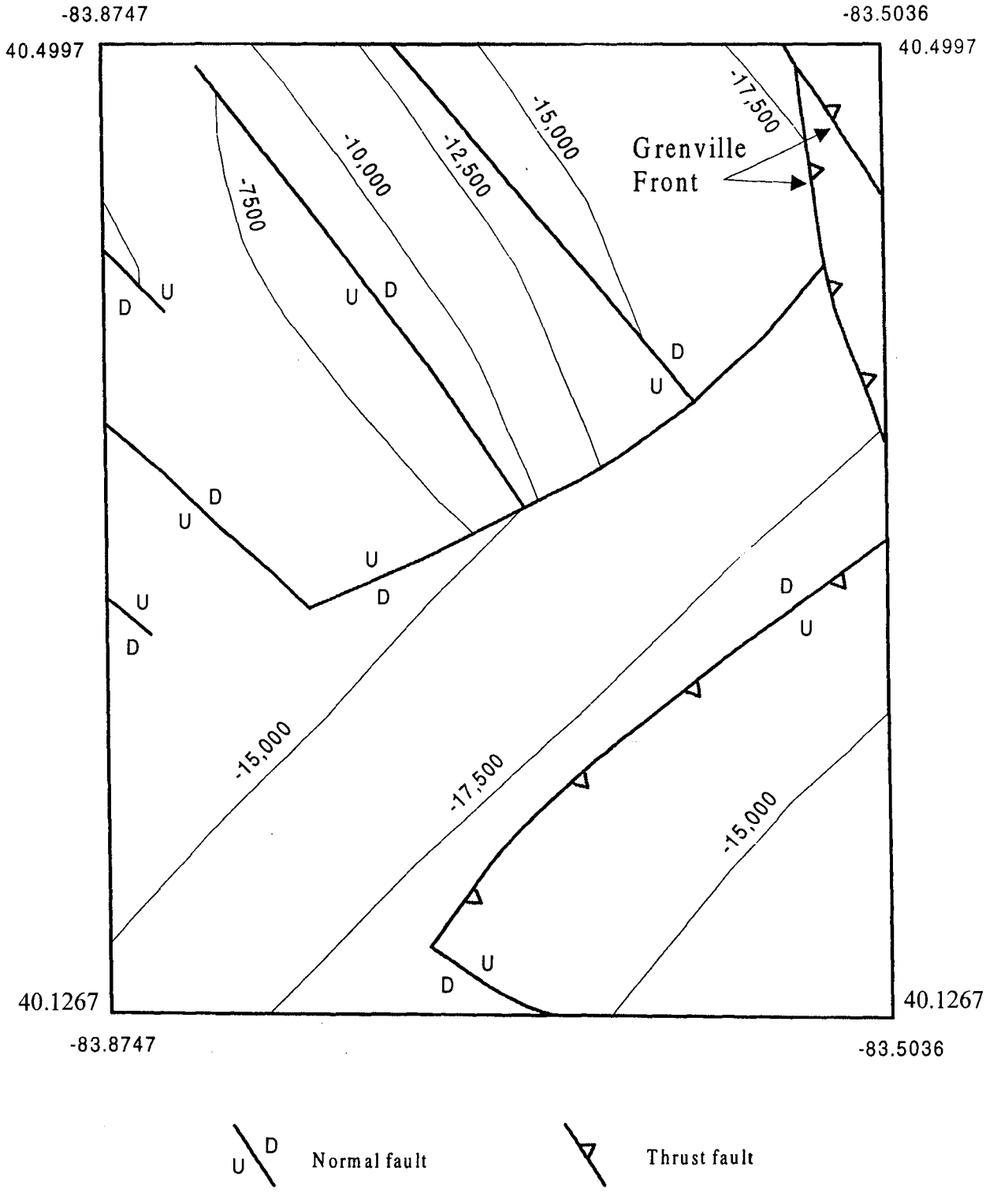

Figure 6 - Structure contour map of the Precambrian Crystalline basement Surface in the Bellefontaine Outlier Study Area. Contour Interval is 2500 ft. (Modified from Steck, 1997).

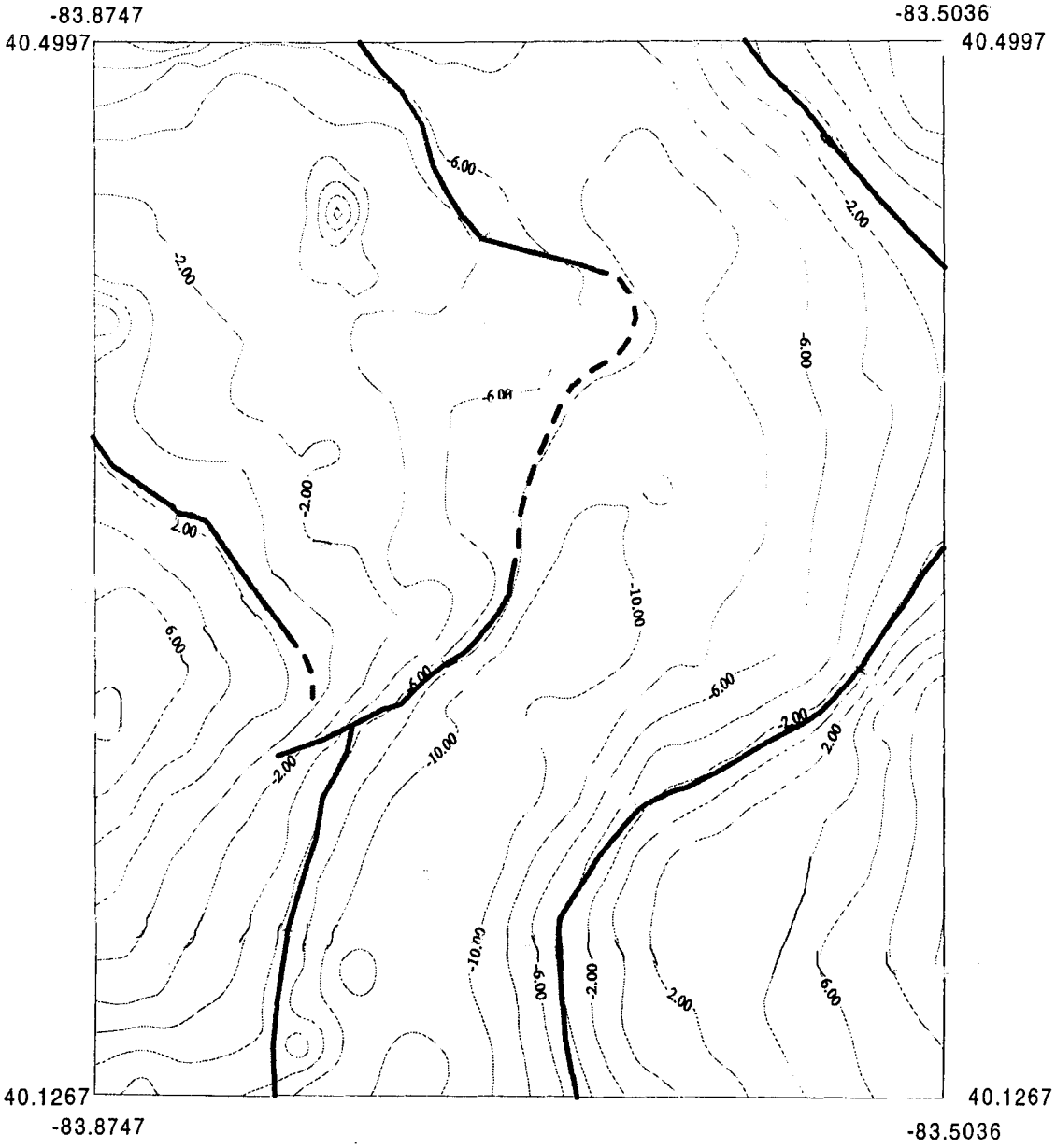

Figure 7- Actual fault location based on Weaver's gravity data. Contour Interval is 2.0 mgal. (Modified from Steck, 1997.)

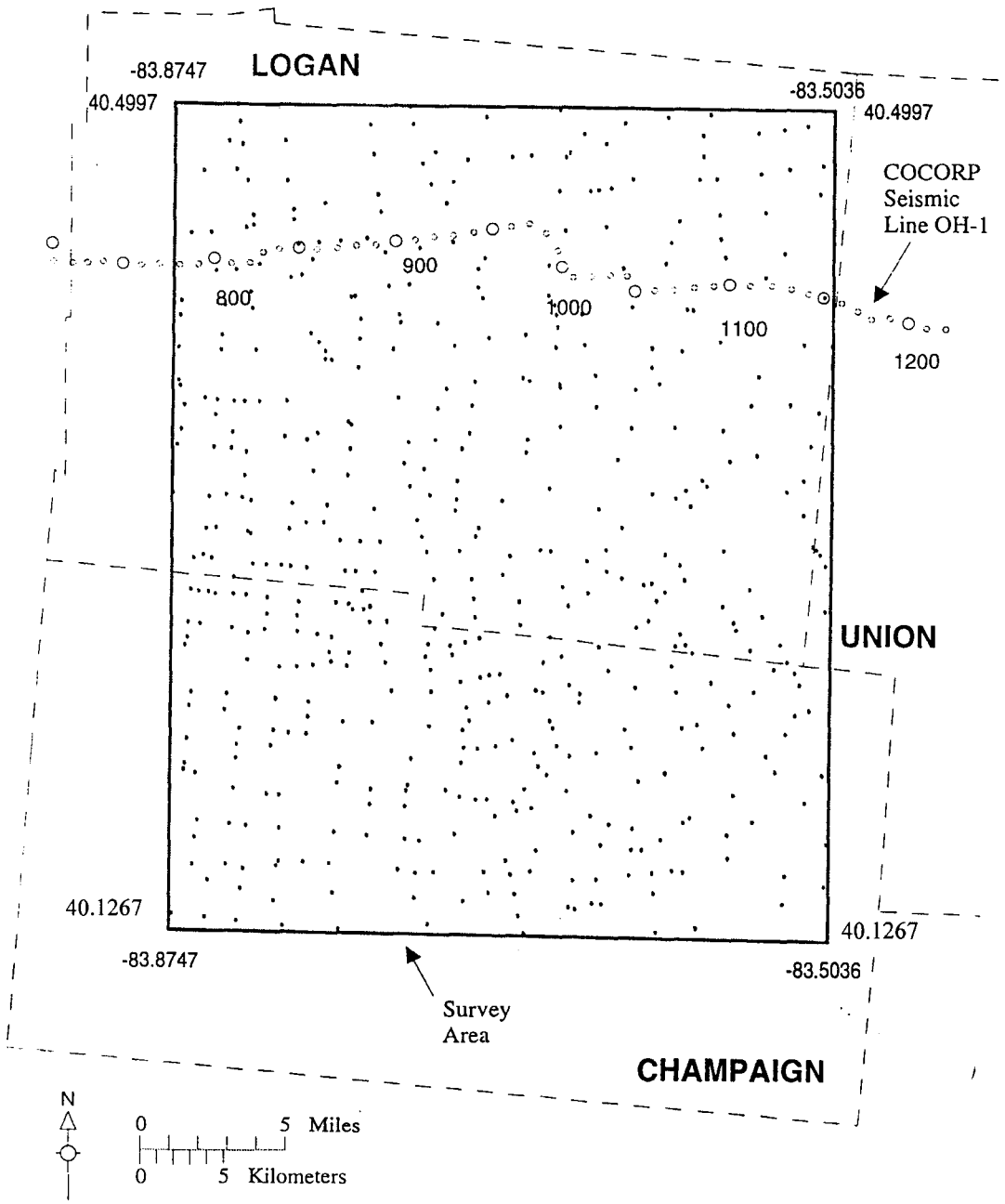

Figure 8 – Map showing the 510 different stations where the magnetic data was gathered. (Modified from Weaver, 1992.)

Total field geomagnetic map with 300 gamma filter.

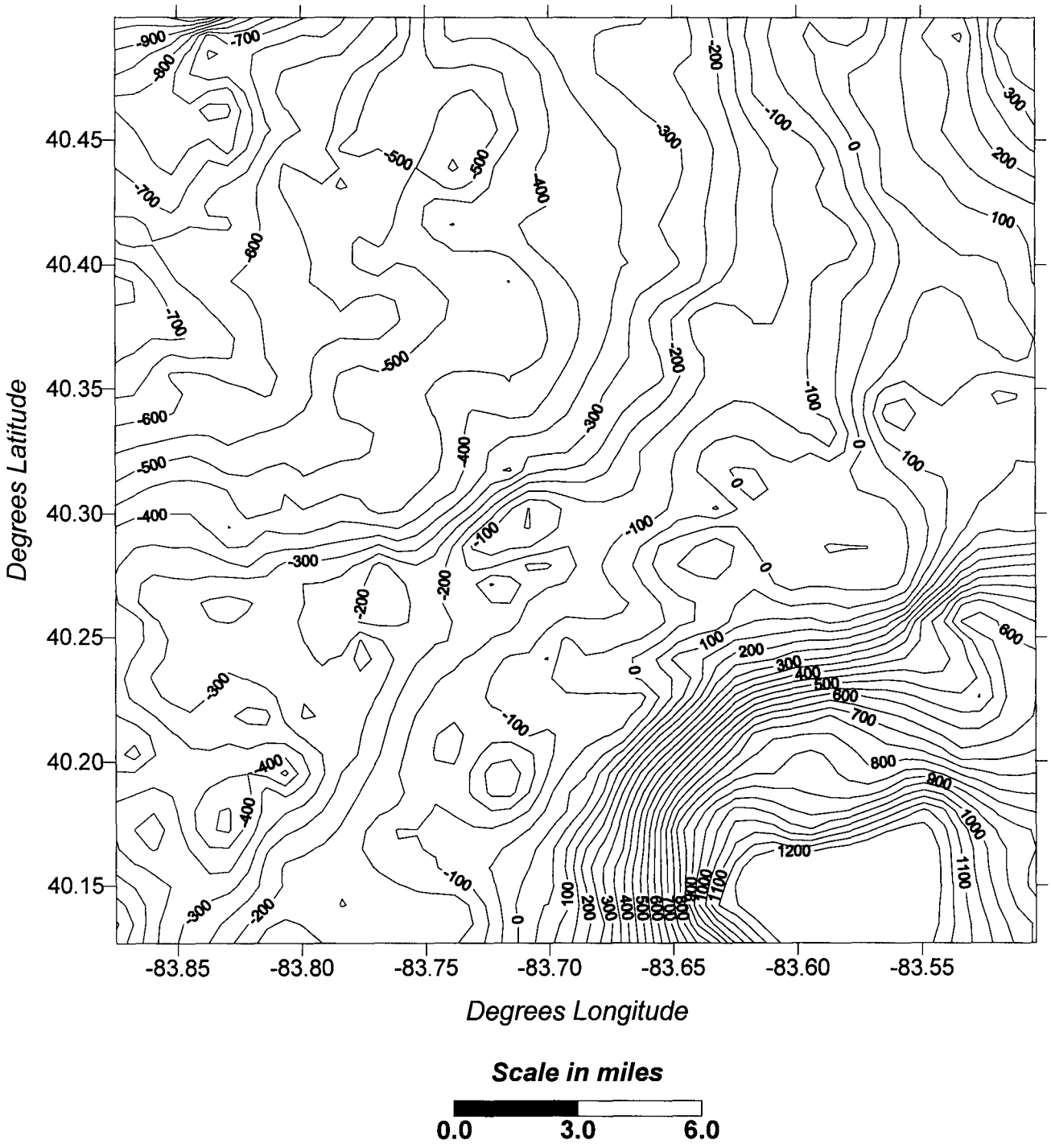

Figure 9 - Complete Magnetic Residual Anomaly map of the Bellefontaine Outlier Study Area. Contour interval is 50 gammas. Modified from Weaver (1992).

Total field geomagnetic map with 300 gamma filter.

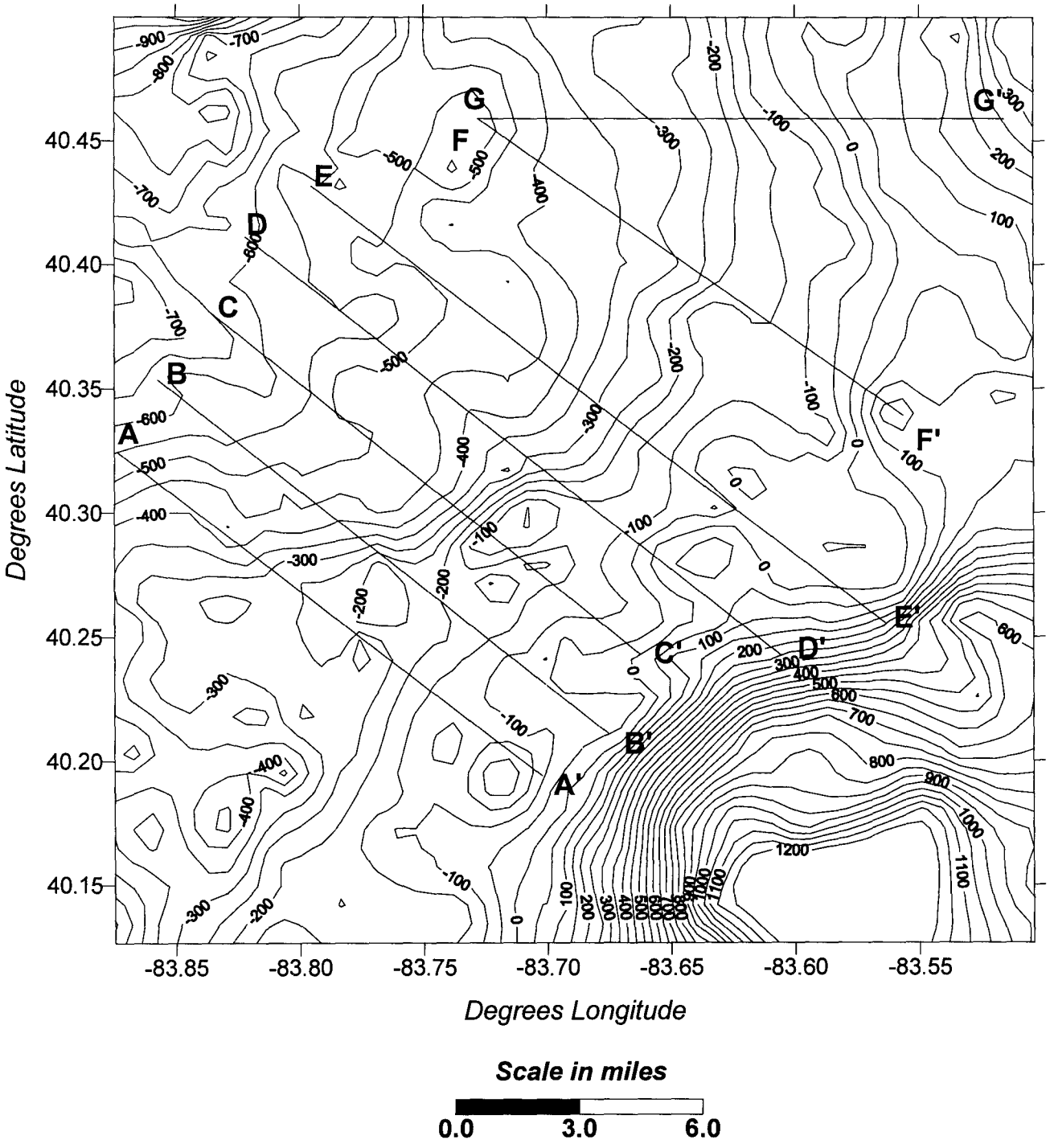

Figure 10 - Complete Magnetic Residual Anomaly map of the Bellefontaine Outlier Study Area with the location of profile traverses. Contour interval is 50 gammas.

All of the profiles were drawn in places previously ignored to explore the faults that were part of the existing interpretation. It was also assumed that since the magnetization of the Paleozoic Strata that overlies the Outlier is much less than that of the Precambrian Crystalline Basement it could be ignored. The location of the faults were identified by the greatest rate of change of the magnetic reading. This was the primary method of determining the location of the faults. It is worth noting that not all of these inflection points precisely locate faults, rather some may merely identify lithology changes. So the rate of change of the magnetic reading could be the result of a fault or of a lithology change in basement rocks.

Formula Derivation

The magnitude of the anomaly can be calculated with the following expression: (Noltimier, 1998)

$$\Delta z = 2J\Delta\theta \qquad \text{(Eqn 1)}$$

where,

$\Delta z = (z_{max} - z_{min})$ = The amplitude change of the residual magnetic anomaly.

J = Magnetization of basement rocks at the fault.

y = The half width of the magnetic anomaly.

The value for y is calculated by taking half the horizontal distance between z_{max} and z_{min}. (There is also a conversion factor involved to change angular distance to kilometers that must be accounted for when determining y. 111.18 km. is roughly equal to 1 degree on the earth's surface. (Noltimier, 1998):

y = 0.5 * (Angular distance in degrees between Δz) * (Conversion factor [111.18 km./degree])

$\Delta\theta$ is found by the formula below:

$$\Delta\theta = \theta_d - \theta_u$$

where,

θ_d, θ_u = The solid angle subtended at surface by downthrown, θ_d, and upthrown, θ_u, fault blocks.

ϕ_d, ϕ_u = The angles (in degrees) between the fault plane to top of the upthrown and downthrown fault blocks thrown at a distance, y, from the fault.

Δh = The throw of the fault.

Equation 1 can be simplified by substituting (θ_d - θ_u) for $\Delta\theta$. In the sample calculations (figure 18) the trigonometric relationships are shown in detail. Below are the equations that relate angles ϕ_u and ϕ_d to the fault throw:

$$\tan\phi_u = (y/h_u)$$
$$\tan\phi_d = (y/h_d)$$

therefore,

$$\phi_u = \tan^{-1} = (y/h_u)$$
$$\phi_d = \tan^{-1} = (y/h_d)$$

The next step is to convert ϕ into θ (radians) through the following conversion:

$$\phi_u * 0.01745 = \theta_u$$
$$\phi_d * 0.01745 = \theta_d$$

Also in equation 1, $\Delta\theta$ is a function of the throw of the fault, Δh. The function for the term, Δh, comes from an expansion of the Taylor Series Expansion for $\tan^{-1} x$, where $(y/h) = x$. The first term of the Taylor Expansion is only term that is considered because as the powers of x increase, the term in higher powers of x become negligible. The angle, ϕ, is taken to be very small (less than 5 degrees) and the following approximation can be made:

$$\tan^{-1} x \approx x,$$

and this leads to the following approximations.

$$\theta_u \approx x_u \approx (y/h_u)$$
$$\theta_d \approx x_d \approx (y/h_d)$$
$$\Delta\theta \approx \theta_u - \theta_d \approx ((y/h_u) - (y/h_d))$$

This effectively simplifies the numbers by removing the tangent function from the formula for ϕ_u and ϕ_d. The next step is to factor, y, out of the expression leaving:

$$\Delta\theta = y(1/h_d - 1/h_u)$$

By manipulating the expression algebraically:

$$\Delta\theta = y[(h_u - h_d)/(h_d h_u)] \qquad \text{(Eqn 2)}$$

Then factor the denominator from the above expression leaving:

$$h_d h_u = (\mathbf{h} + \Delta h/2)(\mathbf{h} - \Delta h/2)$$

And simplifies to:

$$h_d h_u = (\mathbf{h}^2 - \Delta h^2/4),$$

where **h** is the mean depth to the top of the Precambrian crystalline basement. Looking at both parts of the expression, $(\mathbf{h}^2 - \Delta h^2/4)$, it can be noted that the term, $\Delta h^2/4$, is smaller than the term $\mathbf{h}^2$. This simplifies the denominator to just $\mathbf{h}^2$.

This simplifies equation 2 into:

$$\Delta\theta = y(\Delta h^2 / \mathbf{h}^2) \qquad \text{(Eqn 3)}$$

Equation 1 then simplifies into:

$$\Delta z = 2Jy(\Delta h^2 / \mathbf{h}^2) \qquad \text{(Eqn 4)}$$

Equation 4 can then be arithmethically rearranged for the fault throw, Δh (Noltimier, 1998).

$$\Delta h = [(\Delta z \mathbf{h}^2)/(2Jy)] \qquad \text{(Eqn 5)}$$

Sample Calculation

The following is a walkthrough sample calculation fault A-1 (Table 1). Table 1 gives the values for all the calculations, but fault A-1 is the only fault throw being calculated in this section. The calculation is also made easier by using the sample calculation diagram (figure 18) and using equation 5 (Noltimier, 1998). The first part is to inspect the profile for possible fault locations. These are where there is a rapid change in slope of the magnetic profile, due to the difference in elevation of the up and down dropped blocks. Then take the z_{min} and z_{max} right off the profile. For fault A-1:

z_{min} = –430 gammas

z_{max} = –230 gammas

$\Delta z = (z_{max} - z_{min})$ = 200 gammas

However, we must change Δz into oersteds so that we can use it in the fault throw equation. The conversion factor is

$10E^{-5}$ oersteds/gamma.

Δz = (200 gammas) * ($10E^{-5}$ oersteds/gamma)

$\Delta z = 2.0E^{-3}$ oersteds

The next step is to find a value for y. This, once again, is found with a conversion. To calculate is we need to find the angular distance (in degrees) between the Z_{min} and Z_{max}, and it is found along the x-axis of the

profile. The difference between these two points in A-1 is 0.043 degrees. The value, y, is calculated with the following equation:

$y = ½ * (\text{angular distance in degrees}) * (\text{conversion factor})$

The conversion factor is changes degrees to kilometers and is 111.18km./degree. The value for y is:

$y = ½ * (0.043) * (111.18 \text{ km./degree})$

$y = 2.41 \text{ km.}$

The last value that needs to be calculated is $\mathbf{h}^2$. To figure it out we must to refer back to (figure 6) so that we can find the depth (from the surface) to the Precambrian Crystalline Basement. This was calculated by overlaying my profiles (figures 11 – 17) on top of this map. The value of h_u (height of the up dropped block) and h_d (height of the down dropped block) were taken from figure 6:

$h_u = -13{,}500 \text{ ft.}$

$h_d = -14{,}500 \text{ ft.}$

These are the values we need to calculate $\mathbf{h}^2$. Since $\mathbf{h}$ is the average depth to the crystalline basement, is value for h is merely:

$\mathbf{h} = (h_u + h_d)/2$

$\mathbf{h}^2 = ((h_u + h_d)/2)^2$

For $\mathbf{h}^2$ converted to km^2:

$\mathbf{h}^2 = ((h_u + h_d)/2) * (.3048 \text{ m.}) * (1\text{km.}/1000\text{m.}))^2$

For fault A-1:

$\mathbf{h}^2 = ((13500 + 14500) * (.3048/1000))^2$

$\mathbf{h}^2 = 17.56\ km^2$

Now we can calculate the fault throw, the only problem is that we really don't know the exact value of the magnetization (J) of these rocks. We must use some approximate values. For each of the fault throws that were calculated, a range of values for J were used (Table 1) to approximate the fault throw within a certain amount of error. The values of J range from $10E^{-1.8}$ to $10E^{-2.2}$ because it is appropriate for that specific rock type. For the Precambrian Crystalline Basement, this would be a type of basalt. Using the range of values for J, there is enough information to apply equation 5:

$$\Delta h = (\Delta z * \mathbf{h}^2)/(2*J*y)$$

for J = $10E^{-2.0}$ oersteds:

$$\Delta h = ((2.0E^{-3})*(17.56)/(2*10E^{-3})*(2.41))$$

$$\Delta h = 0.73\ km.$$

By using a range of values for the magnetization, the throw of the fault changes accordingly.

Fault number	Z min gammas	Z max gammas	ΔZ oersteds	ang. dist degrees	y (km.)	h^2 (km^2)	J oersteds	ΔH (km.)
A1	-430	-230	2.00E-03	0.043	2.41	17.56	10E-1.8	0.4604
	-430	-230	2.00E-03	0.043	2.41	17.56	10E-2.0	0.7297
	-430	-230	2.00E-03	0.043	2.41	17.56	10E-2.2	1.1564
A2	-290	-10	2.80E-03	0.038	2.13	20.90	10E-1.8	0.8680
	-290	-10	2.80E-03	0.038	2.13	20.90	10E-2.0	1.3757
	-290	-10	2.80E-03	0.038	2.13	20.90	10E-2.2	2.1803
B1	-485	-210	2.75E-03	0.036	1.92	4.49	10E-1.8	0.2023
	-485	-210	2.75E-03	0.036	1.92	4.49	10E-2.0	0.3207
	-485	-210	2.75E-03	0.036	1.92	4.49	10E-2.2	0.5082
B2	-225	-65	1.60E-03	0.0604	3.23	20.90	10E-1.8	0.3268
	-225	-65	1.60E-03	0.0604	3.23	20.90	10E-2.0	0.5180
	-225	-65	1.60E-03	0.0604	3.23	20.90	10E-2.2	0.8209
C1	-595	-505	9.00E-04	0.0315	1.75	4.49	10E-1.8	0.0730
	-595	-505	9.00E-04	0.0315	1.75	4.49	10E-2.0	0.1157
	-595	-505	9.00E-04	0.0315	1.75	4.49	10E-2.2	0.1833
C2	-480	-95	3.85E-03	0.055	3.05	11.76	10E-1.8	0.4685
	-480	-95	3.85E-03	0.055	3.05	11.76	10E-2.0	0.7425
	-480	-95	3.85E-03	0.055	3.05	11.76	10E-2.2	1.1768
D1	-375	-125	2.50E-03	0.04	2.73	12.50	10E-1.8	0.3606
	-375	-125	2.50E-03	0.04	2.73	12.50	10E-2.0	0.5715
	-375	-125	2.50E-03	0.04	2.73	12.50	10E-2.2	0.9058
D2	-125	20	1.45E-03	0.028	1.91	28.45	10E-1.8	0.6800
	-125	20	1.45E-03	0.028	1.91	28.45	10E-2.0	1.0778
	-125	20	1.45E-03	0.028	1.91	28.45	10E-2.2	1.7081
E1	-465	-25	4.40E-03	0.088	4.82	15.70	10E-1.8	0.4525
	-465	-25	4.40E-03	0.088	4.82	15.70	10E-2.0	0.7171
	-465	-25	4.40E-03	0.088	4.82	15.70	10E-2.2	1.1366
F1	-360	-160	2.00E-03	0.043	2.44	17.95	10E-1.8	0.4643
	-360	-160	2.00E-03	0.043	2.44	17.95	10E-2.0	0.7359
	-360	-160	2.00E-03	0.043	2.44	17.95	10E-2.2	1.1664
G1	-535	-345	1.90E-03	0.055	3.12	20.90	10E-1.8	0.4016
	-535	-345	1.90E-03	0.055	3.12	20.90	10E-2.0	0.6365
	-535	-345	1.90E-03	0.055	3.12	20.90	10E-2.2	1.0089

Table 1 – Calculation of all the fault throws of all profiles with varying values for the (J) magnetization of the rocks.

Results

All of the major faults in this study were constructed from a combination of my magnetic profiles and Steck's fault locations (1997). Steck's fault locations were only used for the faults located outside the profiles' area. This refers to the faults in the northeast and southeast corners of the map (figure 20). The location of the faults was not only determined by the numerical data, but also using common sense. Most all of the plots showed a large increase in the magnetic value when approaching the southeastern edge. The presence of a fault seemed likely, but since Z_{max} was still undetermined, the fault's location would not be correct. The same holds true for profile G-G' (figure 17), in the northeast corner and the location of that fault.

Profile A (Figure 11)

There are definitely two very distinct faults that are easily visible upon inspection of the profile. A sample calculation of the first fault (A-1) is given in figure 18. It also appears that there is another fault towards the southeast edge of the profile. However there is not enough data to properly place one from the data gathered in the profile. It does appear on figure 20 because of the data that was collected by Steck (1997). Fault A-2 appears to be an important fault, in my opinion. Figure 20 shows the direction of the fault in the southwest corner.

Profile B (Figure 12)

Two faults are definitely visible in this profile, like in profile A (figure 11). B-1's location was probably the hardest fault to place. Due to the interpretation of faults in figure 7, fault B-1 was placed as part of the southeast trending fault that is found along the western edge of the study area. It seemed reasonable location for the fault and correlates with Steck's interpretation (1997). Fault B-2 seems to be a part of the same fault that A-2 sits on. Once again, there is a sense of another fault at the southeastern edge of the profile. However, a lack of magnetic data outside the profile, prevented me from calculating it's correct location.

Profile C (Figure 13)

Table 1 contains the projected fault throws of faults C-1 and C-2. However, after finding the fault throws of the two faults, it shows that the minimum displacement of fault C-1 is only 0.13 km. This "fault" (C-1) is most likely not a fault at all. It is most likely an anomalous reading and just could result from a lithology change or the presence of are ore body of some type. Fault C-2 is easily distinguishable from figure 13, by the ΔZ of around 400 gammas. It correlates well with the faults given in figure 7.

Profile D (Figure 14)

Table 1 also shows the calculations for two faults (D-1, D-2). Fault D-1 is placed in a reasonable location and correlates with fault interpretation given in figure 7. Fault D-2 I was discarded, not because of it not being a fault at the southeastern edge of the profile, but that the fault wasn't placed in the right location. The sudden decrease in the magnetic reading (figure 14) is about 0.2 degrees (along the profile) and is anomalous and caused me to use a lower Z_{max}. However, since the Z_{max} climbs very fast towards the southeastern edge of the profile, I wasn't able to make a positive location of the fault. Steck's interpretation (1997) accurately represents the proper location of this fault.

Profile E (Figure 15)

There only appears to be one fault present in this profile. Fault E-1 appears to fit along the same fault as D-1 and C-2. This fault seems to trend the magnetic profile. There does appear to be a fault at the eastern side of the profile, but as before there is a lack data from outside the profile line to calculate and exact location.

Profile F (Figure 16)

As in profile E, there seems to be only one fault present (fault F-1) and appears to be a part of the same fault that E-1, D-1, and C-2 are located on. The location of F-1 correlates very well, with the location of the fault in figure 7.

Profile G (Figure 17)

While this profile has the appearance of a smooth profile, with no faults, it might be worthwhile to investigate the sharp rise in the magnetic readings at the northwestern side of the profile. With a fault throw ranging from (0.4 –1.0 km.), it was an important find. This is the correlating factor to the fault interpretation in figure 7, and it shows that the fault that runs through C-2, D-1, E-1, and F-1 does in fact find it's way to the north and off the top of the study area.

Profile Along A - A'

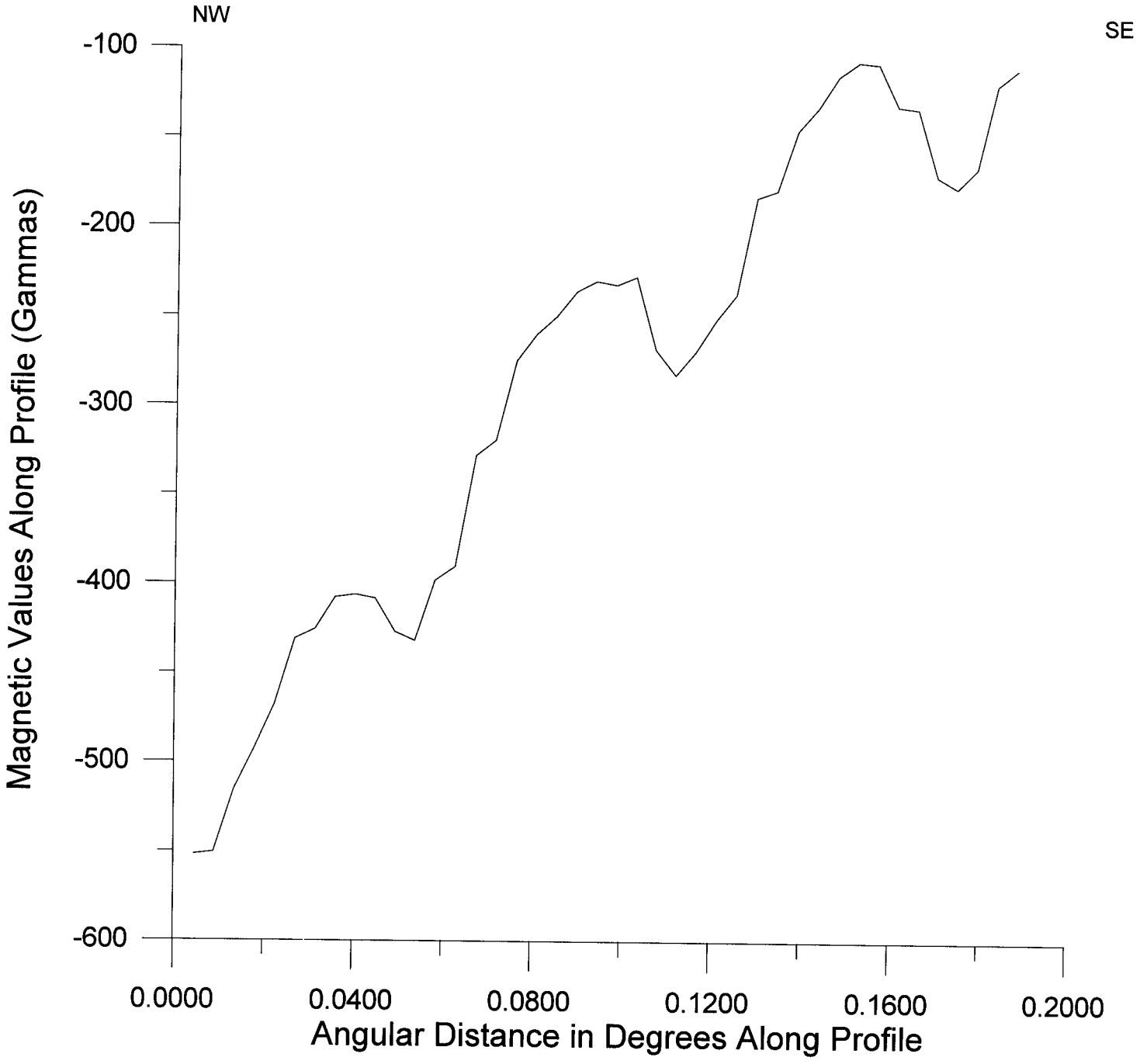

Figure 11 - Range of Magnetic Values along the Profile Traverse A - A'.

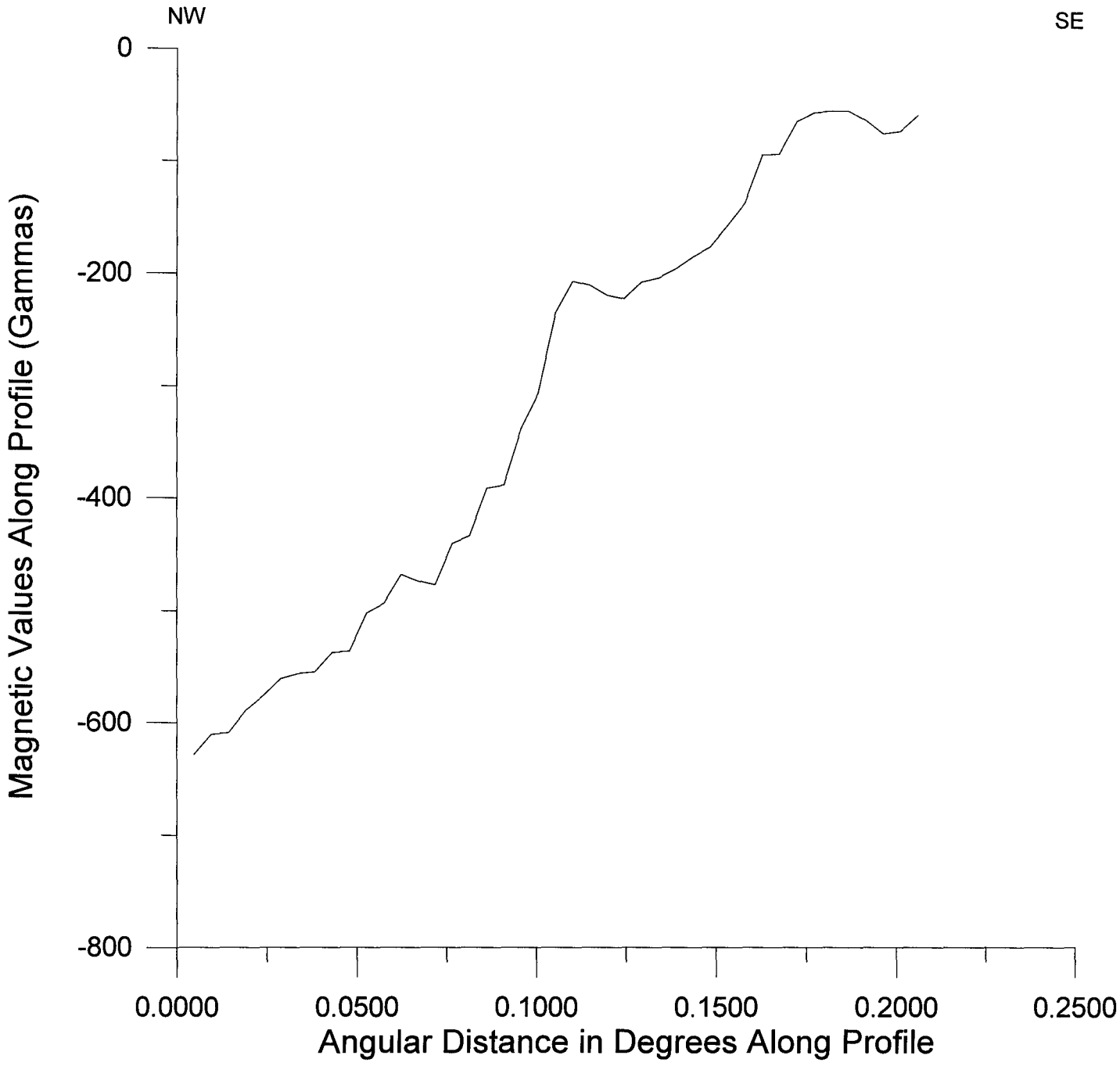

Figure 12 - Range of Magnetic Values along the Profile B - B'.

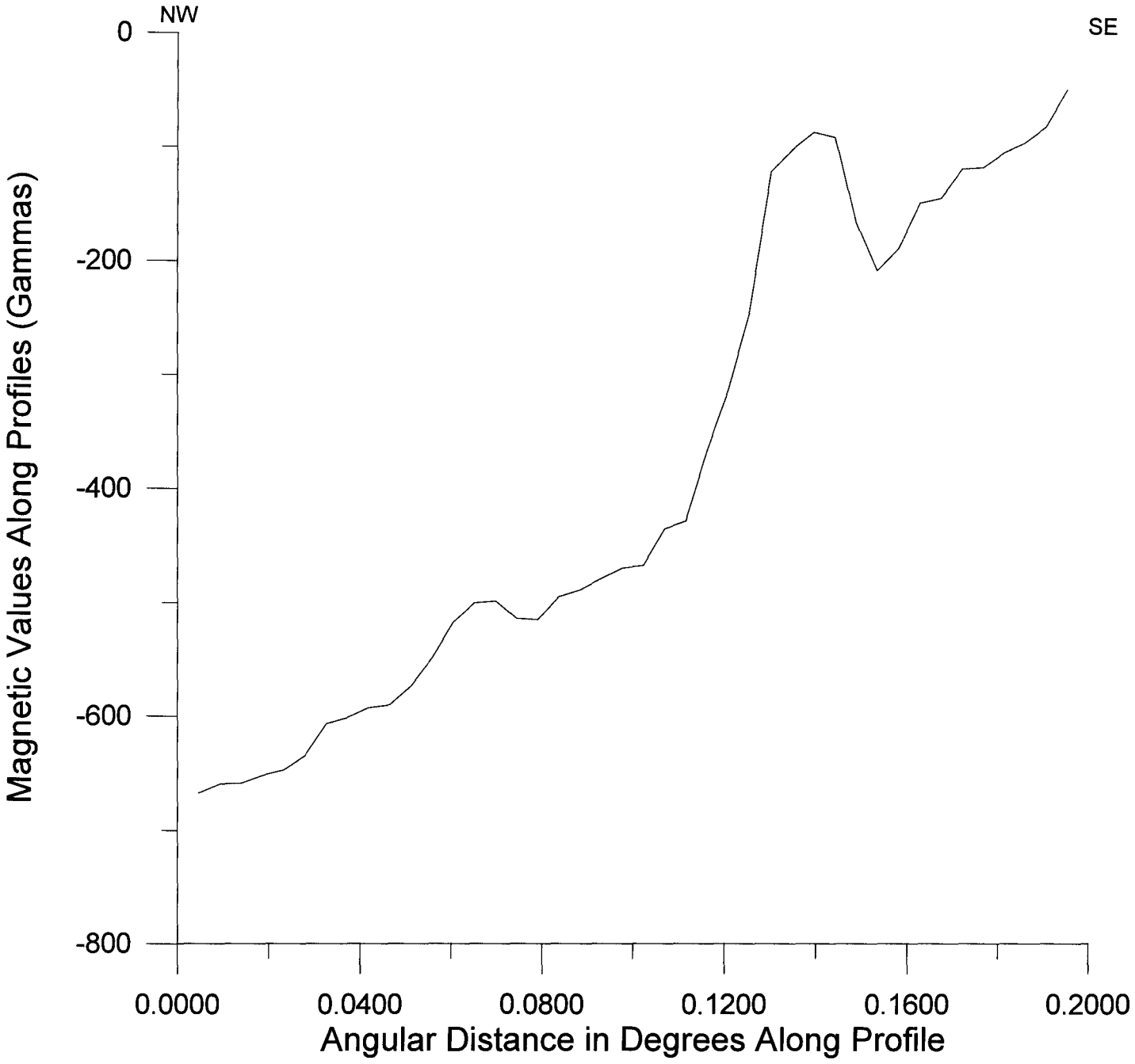

Figure 13 - Range of Magnetic Values along Profile Traverse C - C'.

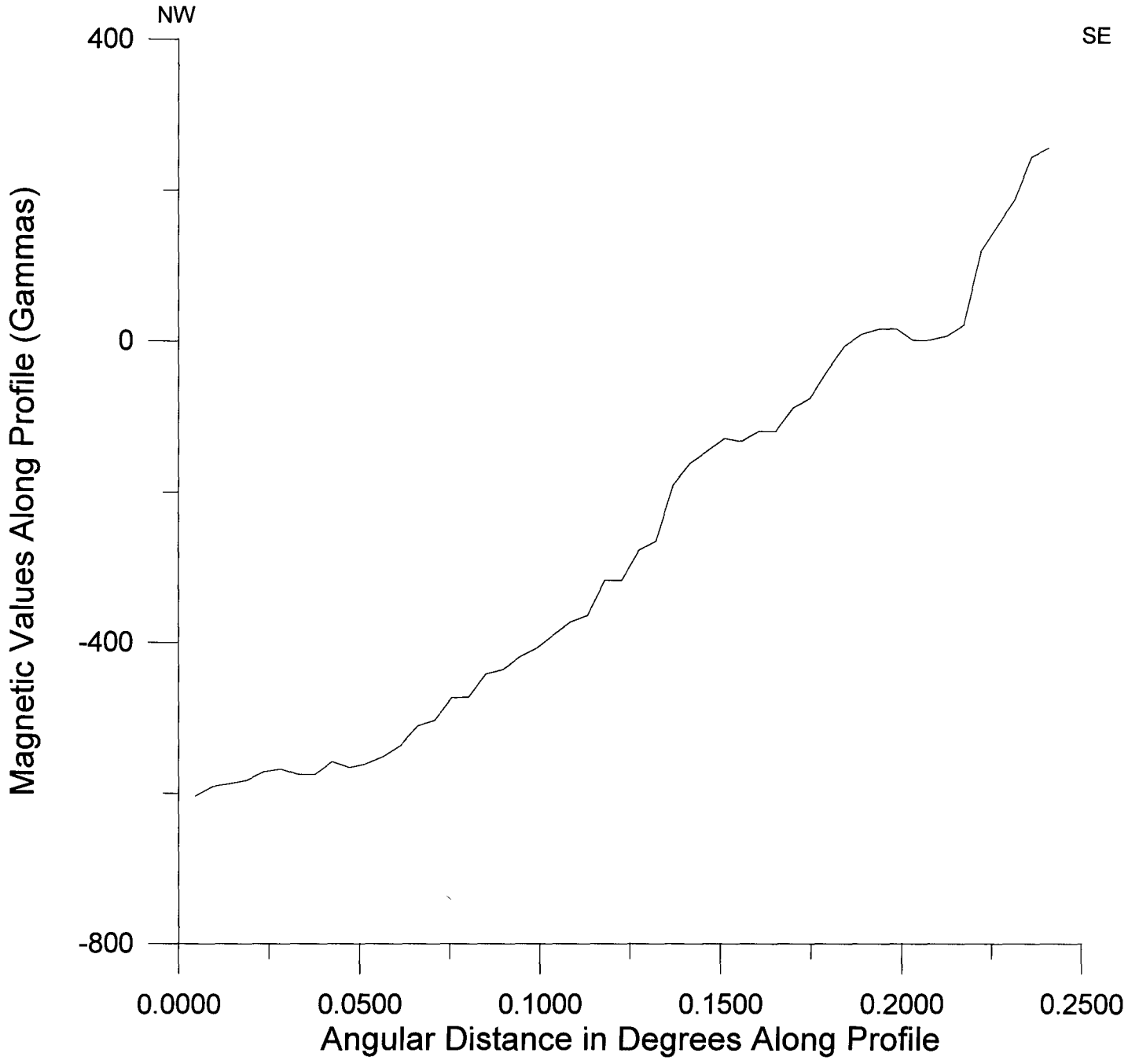

Figure 14 - Range of Magnetic Values along the Profile Traverse D - D'.

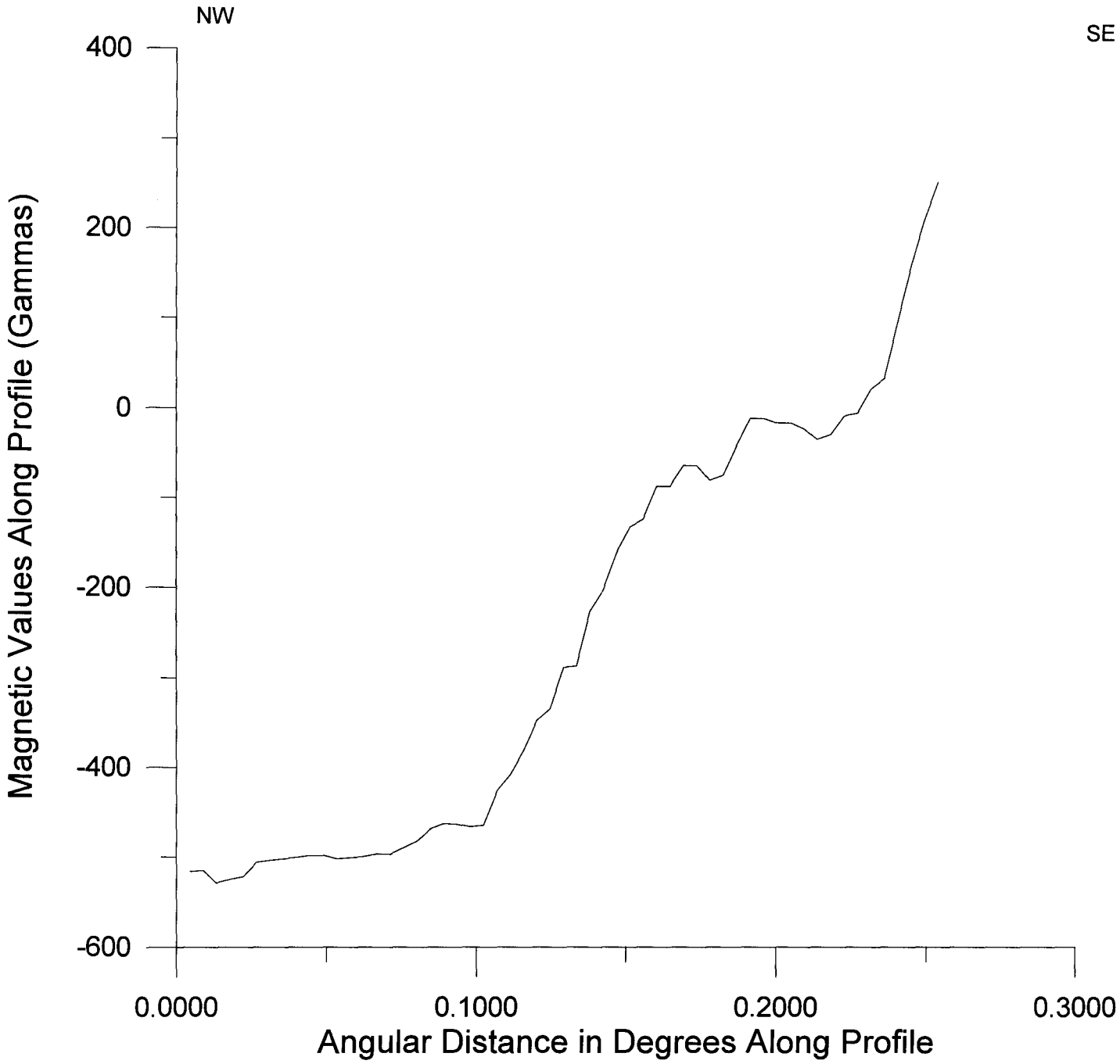

Figure 15 - Range of Magnetic Values along the Profile Traverse E - E'.

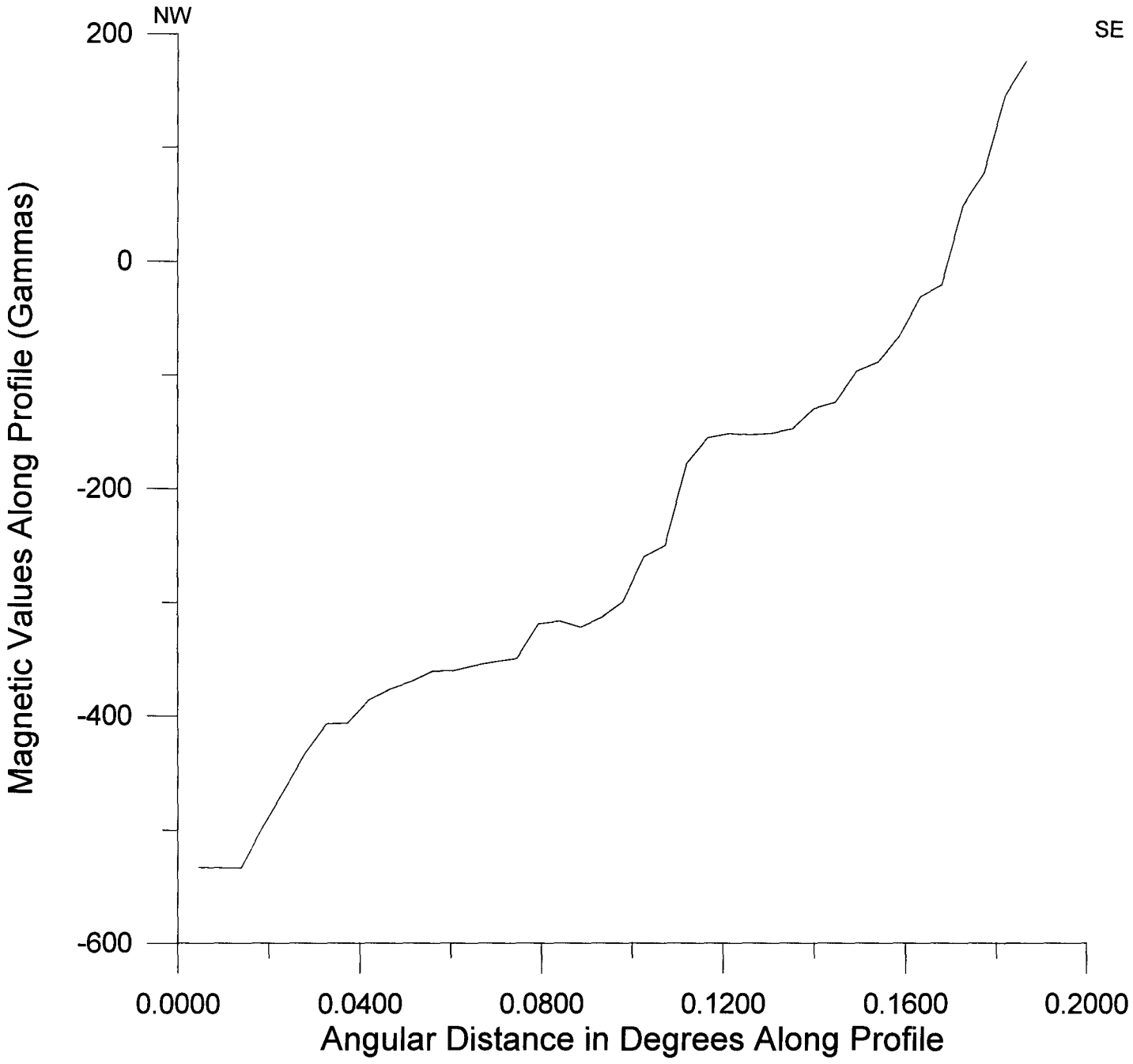

Figure 16 - Range of Magnetic Values along the Profile Traverse F - F'.

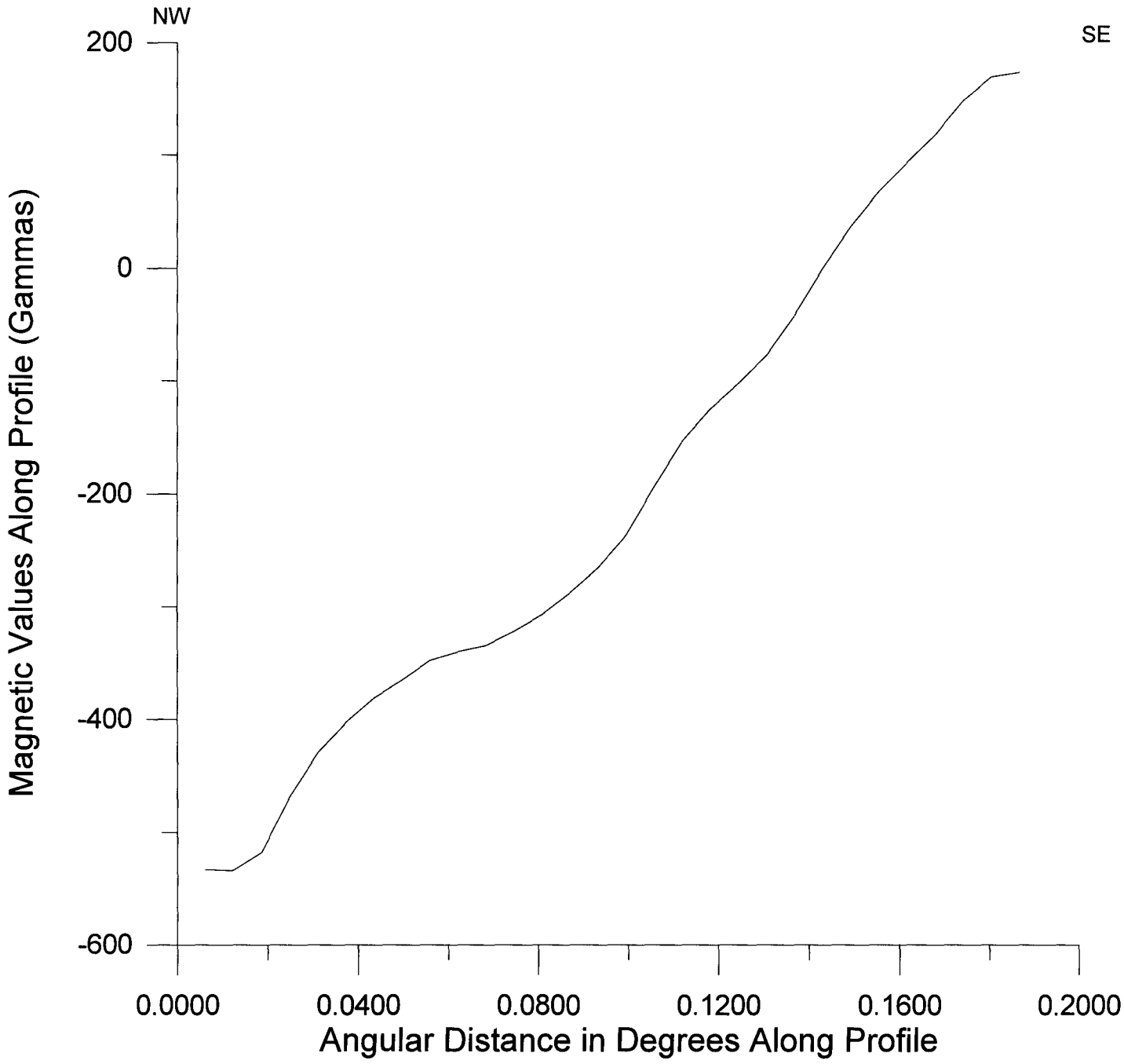

Figure 17 - Range of Magnetic Values along the Profile Traverse G - G'.

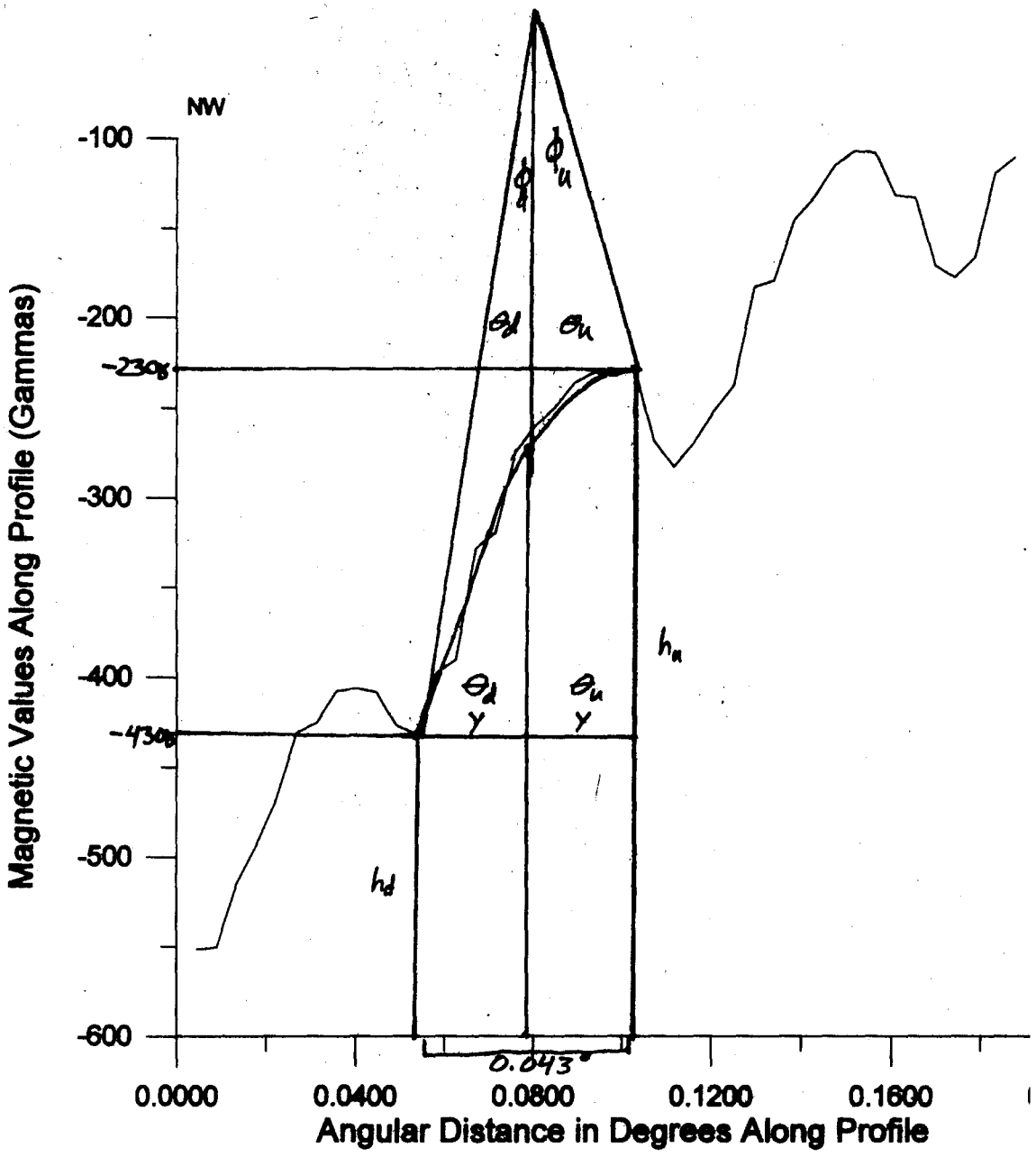

Figure 18 – Sample calculation of the fault A-1 and all of the variables and their Trigonometic relationships

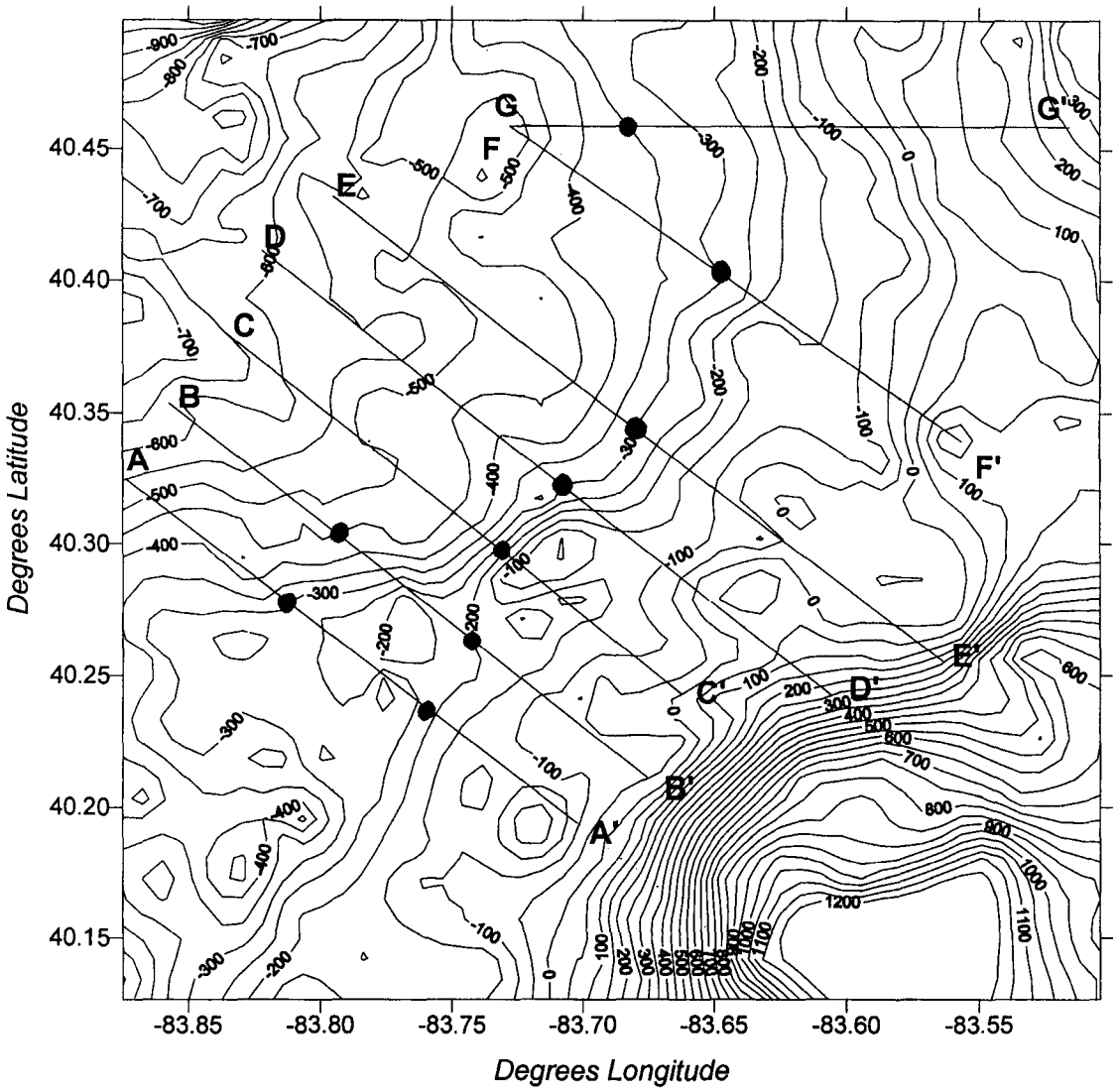

Figure 19 – Location of the probable fault Placements. (Denoted by black dots). Contour interval is 50 gammas.

INTERPRETATIONS AND CONCLUSIONS

The locations and orientations of the faults seems to correlate very nicely to the interpretations given by Steck, (1997). The objective was to test Steck's interpretation of the area (based on gravity) and his fault locations with respect to Drahovzal et al. (1992). I can find no real problems Steck's interpretation. All of my projected fault locations seemed to match up reasonably well to his interpretations. The other part of the objective was to see if I could add anything to his interpretation. If feel that the only part that I made better is that the location of the faults in the southwestern part of the study area is a lot clearer. I feel that I have accurately place the correct locations of these faults. Another section that did become clearer was the section of the fault that ran through profiles F (figure 16) and profile G (figure 17).

I did not get to really explore any of the faults in the northeast or southeast corners of the map, however I feel that those faults are present. I would have probably been able to place them in relatively the same area that Steck did if my profile lines would have given me enough information to accurately locate them.

As to the interpretation of the geology of the area, I have no information to say that the latest interpretation (Noltimier et al, 1998) warrants a new and different explanation at this time.

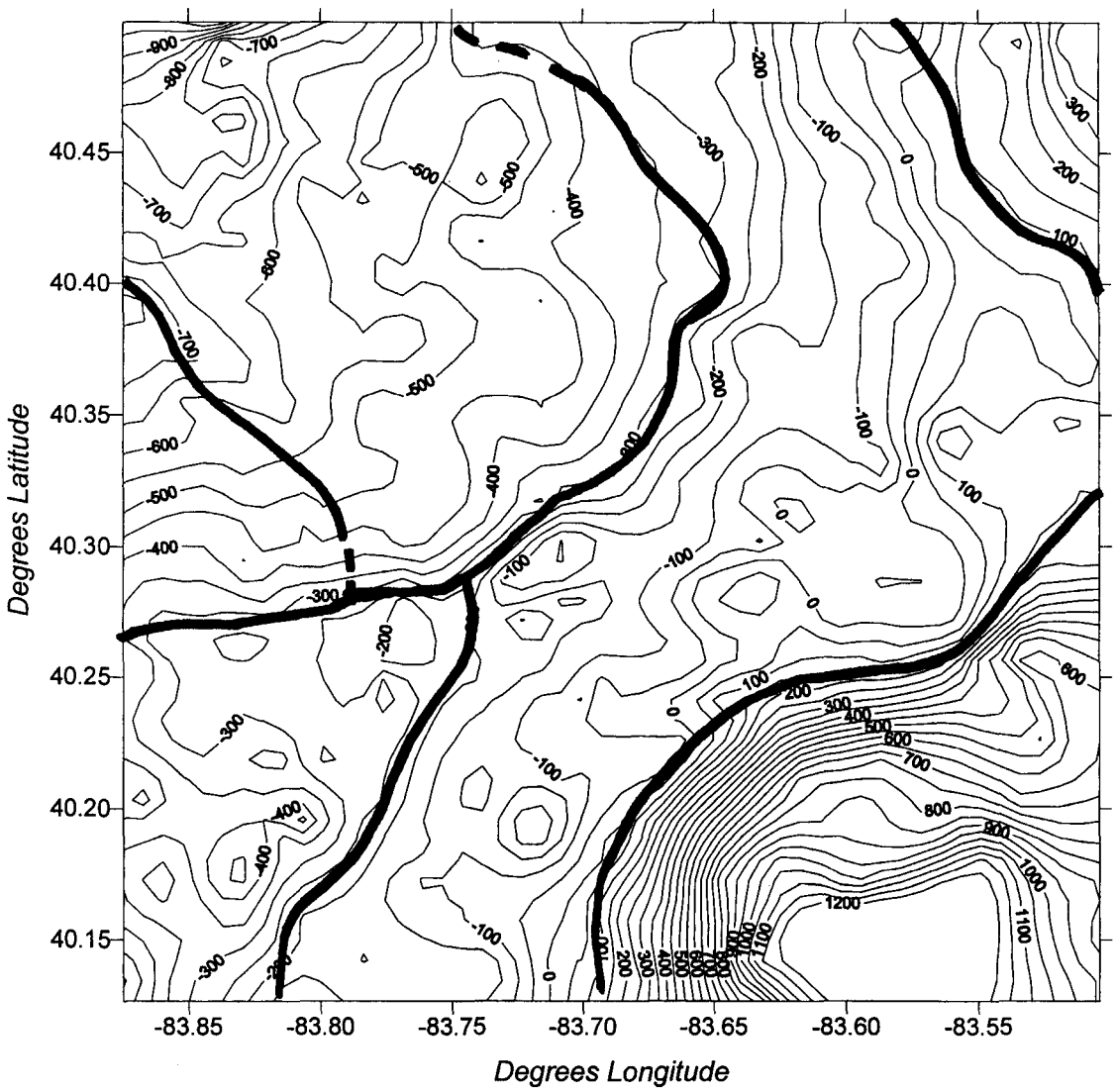

Figure 20 –Location of all faults in the Study area.

REFERENCES CITED

Drahovzal, J. A., D. C. Harris, L. H. Wickstrom, D. Walker, M. T. Baranoski, B. Keith, and L. C. Furer, The east continent rift basin: a new discovery, Ohio Geological Survey Information Circular 57, 1992.

Hansen, M. C., "How the world was made" - the COCORP traverse across Ohio, Ohio Geology Newsletter, Winter 1989.

Hansen, M. C., Campbell Hill - Ohio's Summit, Ohio Geology, Winter 1997, p. 1, 3-5, 1997.

Hansen, M. C., The Geology of Ohio - The Precambrian, Ohio Geological Survey Newsletter, Winter, 1996.

Hoffman, P.F. United Plates of America, the birth of a craton, Ann. Revs. Earth Planet Sci., v. 16, 1988.

Lucius, J. E., and Ralph R. B. Von Frese, Aeromagnetic and gravity constraints on the crustal geology of Ohio, Geol. Society of America Bulletin, v.100, p.104-116, 1988.

Noltimier, H. C., Geological Sciences 693 course notes, 1998.

Noltimier, H. C., Christian D. Steck, Kelley J. Kaltenbach, and Lawrence J. Wickstrom, Basement fault displacement below the Bellefontaine Outlier, Logan, Champaign, and Union Counties, Ohio, Interpreted from a nine quadrangle gravity ang magnetic survey and the Ohio COCORP profile, GSA 1998 North-Central Annual Meeting, Columbus Abst. with programs, BTH 21, A-1022, p.64, 1998.

Steck, C. D., Correlation of Gravity Anomalies with Precambrian Crystalline Basement, Bellefontaine Outlier, Ohio: Bachelors Thesis (unpublished), The Ohio State University, 1997.

Steck, C. D., Lawrence H. Wickstrom, Michael C. Hansen, E. Mac Swinford, and Hallan C. Noltimier, Structural evolution of the Bellefontaine Outlier, Ohio, Ohio Geological Society, 5th annual technical symposium, Akron, Ohio, 1997.

Weaver, J. P., A detailed gravity and magnetic survey of the Bellefontaine Outlier, Logan County, Ohio, Master's Thesis (unpublished), The Ohio State University, 1994.

Wickstrom, L. H., A new look at Trenton (Ordovician) structure in northwestern Ohio, Northeastern Geology, v.12, no.3, 103-113, 1990.

APPENDIX

List of the Magnetic Residual Anomaly Readings. Includes the latitude, longitude, and the magnetic residual with a 300 gamma filter from all stations (510) in the Bellefontaine Oultier Study Area, from Weaver (1992).

Appendix continued

Longitude	Latitude	Magnetic Residual (in gammas)
-83.7308	40.3680	-160.78443120
-83.7814	40.4428	-121.71153440
-83.8397	40.4997	-835.38008592
-83.8386	40.4919	-346.49052114
-83.8444	40.4831	-429.08533586
-83.8369	40.4817	-340.42267067
-83.7814	40.4428	-113.91153440
-83.7814	40.4428	-113.59793440
-83.7308	40.3680	-160.78443120
-83.7308	40.3680	-160.78443120
-83.7814	40.4428	-123.59793440
-83.8586	40.4697	-490.57069652
-83.8403	40.4706	-367.93052196
-83.8339	40.4656	-584.70505136
-83.8114	40.4656	-289.47483636
-83.8078	40.4525	-337.75571370
-83.7814	40.4428	-118.09843440
-83.8125	40.4836	-316.36757060
-83.7653	40.4906	-294.58610880
-83.7633	40.4775	-167.16203570
-83.7606	40.4594	-165.18865980
-83.7814	40.4428	-132.99423440
-83.7592	40.4517	-138.88467250
-83.7814	40.4386	-258.01746620
-83.7933	40.4378	-313.84459200
-83.8050	40.4372	-220.33263120
-83.7900	40.4553	-281.98429130
-83.7814	40.4428	-114.91013440
-83.8653	40.4417	-414.69587190
-83.8542	40.4419	-484.66597670
-83.8347	40.4444	-386.92382620
-83.8308	40.4500	-458.06435320
-83.8306	40.4456	-483.15903000
-83.8078	40.4481	-289.13196130
-83.7814	40.4428	-131.02663440
-83.7564	40.4336	-191.19071120
-83.8514	40.4247	-429.83424430
-83.8403	40.4253	-339.31751750
-83.7814	40.4428	-108.61593440
-83.7308	40.3680	-160.76573120
-83.7308	40.3680	-160.78443120
-83.7814	40.4428	-117.75353440
-83.8272	40.4275	-323.98955630
-83.8092	40.4219	-275.20182670
-83.8031	40.4233	-247.04800670
-83.7967	40.4300	-192.09871180
-83.7814	40.4428	-137.22913440
-83.7542	40.4183	-176.75574110
-83.7708	40.3817	-315.83160890
-83.7514	40.3900	-214.34128560
-83.7703	40.3947	-185.02005490
-83.7697	40.4036	-197.70073940
-83.7814	40.4428	-139.00633440
-83.7753	40.4136	-194.27273180
-83.7731	40.4139	-213.28452930
-83.7856	40.3847	-233.33141110
-83.7892	40.3850	-293.00076180
-83.7892	40.3886	-220.21087740
-83.7814	40.4428	-147.00153440
-83.7975	40.3969	-270.51210990

Appendix continued

Longitude	Latitude	Magnetic Residual (in gammas)
-83.7931	40.3928	-224.50777620
-83.8717	40.3900	-495.42852180
-83.7814	40.4428	-117.76873440
-83.7308	40.3680	-160.78363120
-83.7308	40.3680	-160.78443120
-83.7814	40.4428	-114.45673440
-83.8717	40.3750	-392.72210680
-83.8481	40.3889	-368.00105430
-83.8478	40.3958	-320.88475300
-83.8286	40.3886	-296.60902500
-83.7814	40.4428	-99.20000000
-83.8708	40.4044	-388.07301560
-83.8703	40.4111	-304.39525930
-83.8461	40.4092	-324.38104260
-83.8306	40.4078	-322.08091620
-83.8317	40.4153	-375.94536310
-83.7814	40.4428	-112.81663440
-83.7308	40.3680	-160.77873120
-83.7308	40.3680	-160.78443120
-83.6881	40.4428	-52.18595620
-83.7428	40.4992	-89.73711440
-83.7411	40.4914	-88.81657880
-83.7358	40.4739	-174.48603510
-83.7286	40.4786	-163.77381500
-83.6881	40.4428	-81.51955620
-83.7308	40.4642	-238.45303140
-83.7181	40.4656	-144.50337500
-83.7100	40.4758	-146.08675180
-83.6994	40.4947	-21.25610630
-83.7217	40.4558	-218.25142360
-83.7181	40.4386	-107.07930800
-83.6881	40.4428	-82.27555620
-83.6850	40.4772	-4.23729120
-83.6742	40.4781	9.23870310
-83.6578	40.4986	-2.98257180
-83.6439	40.4878	28.75974560
-83.6522	40.4794	66.18389380
-83.6544	40.4775	32.35156490
-83.6881	40.4428	-68.41955620
-83.6314	40.4833	92.76766510
-83.6286	40.4633	107.05047630
-83.6356	40.4625	44.01543510
-83.6881	40.4428	-59.68035620
-83.7308	40.3680	-160.77243120
-83.7308	40.3680	-160.78443120
-83.6881	40.4428	-83.86675620
-83.6403	40.4622	56.26699760
-83.6314	40.4461	56.48832630
-83.6578	40.4619	11.65402890
-83.6544	40.4444	-38.08495000
-83.7667	40.4400	-252.59170180
-83.7369	40.4358	-273.60620000
-83.7428	40.4192	-61.32023440
-83.7481	40.4058	-189.73451920
-83.7475	40.4022	-181.42329120
-83.7264	40.4017	-165.08791130
-83.6881	40.4428	-62.96835620
-83.7167	40.3917	-212.32911750
-83.6972	40.3956	-104.73315640
-83.7008	40.4133	-54.78653250

Appendix continued

Longitude	Latitude	Magnetic Residual (in gammas)
-83.7036	40.4183	-61.51932870
-83.7036	40.4267	-149.80806510
-83.6881	40.4428	-58.10535620
-83.7308	40.3680	-160.79583120
-83.7308	40.3680	-160.78443120
-83.6881	40.4428	-65.64915620
-83.6997	40.4314	-74.71776320
-83.6639	40.4286	-33.55801120
-83.6639	40.4150	-42.13988560
-83.6603	40.4106	17.12044120
-83.6592	40.4064	-28.73185120
-83.6447	40.4069	16.24797130
-83.6881	40.4428	-61.45875620
-83.7050	40.3758	-162.43458180
-83.6781	40.3778	-71.13235120
-83.6744	40.3764	-47.13960200
-83.6572	40.3750	77.66877620
-83.6369	40.3792	206.16434420
-83.6881	40.4428	-69.60755620
-83.6767	40.3975	-66.33309930
-83.6586	40.4008	-54.99798120
-83.6594	40.3917	5.05611670
-83.6431	40.3931	9.57884750
-83.6881	40.4428	-62.69475620
-83.7308	40.3680	-160.79483120
-83.7308	40.3680	-160.78443120
-83.5425	40.4350	433.37907000
-83.6164	40.4678	207.93705060
-83.6211	40.4928	205.27991180
-83.5969	40.4956	311.49129980
-83.5731	40.4969	280.67712770
-83.5772	40.4878	290.97850740
-83.5772	40.4786	357.52618060
-83.5425	40.4350	401.85797000
-83.5447	40.4711	408.31744310
-83.5461	40.4892	477.30107740
-83.5322	40.4906	433.10205860
-83.5189	40.4925	670.32826690
-83.5100	40.4750	662.83218500
-83.5292	40.4733	512.22405390
-83.5425	40.4350	420.58577000
-83.7308	40.3680	-160.78023120
-83.7308	40.3680	-160.78443120
-83.5425	40.4350	387.92257000
-83.5903	40.4494	221.53368640
-83.5792	40.4681	344.52274310
-83.5694	40.4683	388.57782810
-83.5678	40.4522	351.20592260
-83.5422	40.4536	448.93469560
-83.5114	40.4622	577.04277820
-83.5036	40.4567	610.15780490
-83.5425	40.4350	432.61707000
-83.6217	40.4278	111.29856440
-83.5947	40.4397	154.69406250
-83.5669	40.4417	343.78356170
-83.5642	40.4333	373.03700390
-83.5978	40.4300	198.34464880
-83.5425	40.4350	416.97997000
-83.5042	40.3944	408.68537080
-83.5203	40.3947	327.83624510

Appendix continued

Longitude	Latitude	Magnetic Residual (in gammas)
-83.5086	40.4161	400.88332750
-83.5419	40.4244	385.79964500
-83.5314	40.4356	440.46589680
-83.5425	40.4350	425.06567000
-83.7308	40.3680	-160.79733120
-83.7308	40.3680	-160.78443120
-83.5425	40.4350	415.28827000
-83.5453	40.3800	384.18403380
-83.6008	40.3758	174.20230500
-83.6050	40.3833	149.32391070
-83.6050	40.3919	137.71749010
-83.5883	40.3911	240.13278870
-83.5669	40.3953	268.53539610
-83.5425	40.4350	402.48447000
-83.5822	40.4094	147.67024380
-83.5856	40.4097	176.67536390
-83.6164	40.4103	129.16460810
-83.5425	40.4350	399.57417000
-83.7308	40.3680	-160.78443120
-83.7308	40.3680	-160.78443120
-83.8133	40.3050	-188.17836320
-83.8708	40.3725	-446.37213570
-83.8683	40.3639	-398.82938010
-83.8569	40.3669	-377.22020750
-83.8697	40.3528	-388.33335260
-83.8722	40.3458	-344.66254060
-83.8133	40.3050	-139.07836320
-83.8508	40.3594	-278.36379060
-83.8500	40.3661	-406.17327810
-83.8406	40.3656	-386.07659000
-83.8347	40.3656	-356.61985140
-83.8264	40.3653	-368.68938690
-83.8133	40.3050	-153.95716320
-83.7933	40.3514	-222.84581760
-83.8108	40.3661	-275.68540130
-83.8119	40.3500	-312.78381260
-83.7992	40.3489	-286.76365370
-83.7953	40.3344	-212.72426860
-83.8133	40.3050	-139.06176320
-83.8517	40.3447	-321.67452050
-83.8419	40.3444	-297.21027500
-83.8411	40.3517	-268.58871510
-83.8336	40.3428	-251.68381320
-83.8342	40.3322	-258.14236300
-83.8739	40.3239	-248.50012250
-83.8133	40.3050	-113.42656320
-83.8747	40.3092	-185.63926700
-83.8556	40.3078	-121.02056620
-83.8542	40.3222	-208.82783300
-83.8133	40.3050	-120.11916320
-83.7308	40.3680	-160.77703120
-83.7308	40.3680	-160.78443120
-83.8133	40.3050	-116.71036320
-83.7761	40.3569	-172.86759430
-83.7744	40.3556	-207.48424520
-83.7761	40.3328	-219.40219820
-83.7750	40.3447	-149.92371870
-83.7614	40.3175	-172.53585310
-83.7875	40.3189	-201.67653190
-83.8133	40.3050	-137.03436320

Appendix continued

Longitude	Latitude	Magnetic Residual (in gammas)
-83.8447	40.3233	-198.39383310
-83.8356	40.3222	-214.97654860
-83.8306	40.3208	-243.01918920
-83.8072	40.3197	-195.55151676
-83.7992	40.3111	-204.94220203
-83.8086	40.3083	-133.39697509
-83.8133	40.3050	-118.53836320
-83.7892	40.3111	-169.88829990
-83.7800	40.3031	-117.97202658
-83.7689	40.3028	-178.88809514
-83.7714	40.2892	-18.27264241
-83.7606	40.2886	-65.55671513
-83.7578	40.3025	-152.81216370
-83.8133	40.3050	-130.81036320
-83.8500	40.3083	-123.59653069
-83.8322	40.3067	-112.94708311
-83.8133	40.3050	-141.00636320
-83.7308	40.3680	-160.78843120
-83.7308	40.3680	-160.78443120
-83.8133	40.3050	-138.90276320
-83.7772	40.2892	-58.47719561
-83.7986	40.2906	-100.03109848
-83.8078	40.2911	-104.10242643
-83.8131	40.2914	-72.66490467
-83.8217	40.2914	-129.90674907
-83.8294	40.2919	-156.08439602
-83.8306	40.3058	-130.10000000
-83.8133	40.3050	-153.16546320
-83.8572	40.2956	-99.75384788
-83.8625	40.2944	-65.77853424
-83.8638	40.2800	-25.37886520
-83.8594	40.2792	-19.43648441
-83.8539	40.2789	-9.07293537
-83.8500	40.2781	-40.95828158
-83.8400	40.2858	-39.01916819
-83.8525	40.2942	-83.79210681
-83.8133	40.3050	-156.80716320
-83.8400	40.2781	-28.18744158
-83.8328	40.2778	-18.87534074
-83.8208	40.2764	-42.84076547
-83.8211	40.2692	51.76293379
-83.8222	40.2625	54.09067870
-83.8039	40.2689	16.95137463
-83.8036	40.2619	35.23986718
-83.8028	40.2750	73.99663380
-83.8133	40.3050	-137.42996320
-83.7308	40.3680	-160.77513120
-83.7308	40.3680	-160.78443120
-83.8133	40.3050	-131.96636320
-83.8653	40.2656	12.76616472
-83.8656	40.2586	-26.95992221
-83.8669	40.2550	-102.43328760
-83.8586	40.2647	45.93944264
-83.8133	40.3050	-131.61756320
-83.7308	40.3680	-160.78843120
-83.7308	40.3680	-161.38443120
-83.8133	40.3050	-148.07386320
-83.8317	40.2611	79.20562589
-83.8408	40.2633	51.37946987
-83.7922	40.2606	81.26759712

Appendix continued

Longitude	Latitude	Magnetic Residual (in gammas)
-83.7844	40.2594	41.58976648
-83.7856	40.2525	90.08224510
-83.7744	40.2525	115.66340990
-83.7567	40.2564	104.49509593
-83.7633	40.2664	151.77144953
-83.8133	40.3050	-159.40386320
-83.7822	40.2747	62.99727824
-83.7753	40.2744	83.43102288
-83.7731	40.2719	103.98830418
-83.7669	40.2722	134.56304694
-83.7633	40.2731	119.18796522
-83.7536	40.2669	70.89706218
-83.7675	40.2800	123.13267500
-83.8133	40.3050	-152.65436320
-83.7308	40.3680	-168.25093120
-83.7483	40.3680	-189.52687620
-83.7258	40.3633	-170.78551889
-83.7272	40.3489	-118.07340357
-83.7333	40.3361	-87.53724843
-83.7447	40.3386	-147.27498653
-83.7425	40.3481	-126.44044658
-83.7308	40.3680	-160.79093120
-83.7064	40.3650	-175.48613060
-83.7211	40.3722	-151.49181560
-83.7308	40.3680	-161.37643120
-83.7308	40.3680	-160.78443120
-83.7119	40.3453	-159.00005964
-83.7078	40.3525	-125.44081370
-83.7142	40.3308	-48.75887999
-83.7147	40.3222	2.04087574
-83.7153	40.3175	-63.94968370
-83.7300	40.3239	-58.23736977
-83.7411	40.3281	-158.42693098
-83.7308	40.3680	-165.64073120
-83.6758	40.3442	9.01014499
-83.6750	40.3500	16.58650000
-83.6569	40.3736	59.58182180
-83.6564	40.3558	22.21525621
-83.6361	40.3650	160.49300560
-83.6625	40.3278	151.43664546
-83.7308	40.3680	-172.95013120
-83.6342	40.3189	292.08104843
-83.6300	40.3003	166.06872796
-83.6406	40.2953	275.37368056
-83.6294	40.2906	399.84349832
-83.6614	40.2994	144.42226848
-83.6672	40.2997	175.99506324
-83.6842	40.2969	181.41619978
-83.7308	40.3680	-160.77543120
-83.7308	40.3680	-160.78443120
-83.6889	40.3219	9.05516098
-83.7036	40.3058	260.44379741
-83.7019	40.3097	133.61261944
-83.7128	40.2989	257.55214403
-83.7272	40.2858	272.35866301
-83.7314	40.2981	49.45668282
-83.7342	40.3053	-51.21596384
-83.7308	40.3680	-175.14823120
-83.7369	40.3128	-118.64317714
-83.7222	40.2703	20.44341916

Appendix continued

Longitude	Latitude	Magnetic Residual (in gammas)
-83.7264	40.2639	133.36046463
-83.7300	40.2567	143.20194569
-83.7314	40.2511	75.90875917
-83.7175	40.2564	100.45617273
-83.7161	40.2522	160.76114355
-83.7308	40.3680	-169.78923120
-83.7089	40.2581	178.09873782
-83.7008	40.2600	169.66525680
-83.7036	40.2694	183.00885968
-83.7042	40.2775	33.06093570
-83.7056	40.2864	206.72440533
-83.7308	40.3680	-160.78773120
-83.7308	40.3680	-160.78443120
-83.6881	40.2883	135.21035191
-83.6789	40.2764	207.88101713
-83.6781	40.2664	176.60281033
-83.6611	40.2608	198.20873741
-83.6544	40.2522	247.47910778
-83.7308	40.3680	-175.55493120
-83.6333	40.2567	290.36052749
-83.6511	40.2750	336.25988560
-83.6397	40.2808	371.94879301
-83.6542	40.2833	336.74660751
-83.7308	40.3680	-182.13343120
-83.5769	40.2947	275.38008444
-83.5856	40.3281	123.86516602
-83.6239	40.3414	215.34662213
-83.6161	40.3558	166.24217241
-83.6142	40.3733	146.23196390
-83.5917	40.3564	212.14440593
-83.5769	40.2947	275.46080870
-83.5828	40.3211	284.18162649
-83.5911	40.3244	263.28451136
-83.6042	40.3261	216.43451297
-83.5764	40.3328	299.64216986
-83.5736	40.3300	310.58091560
-83.5769	40.2947	282.88230870
-83.7308	40.3680	-160.79943120
-83.7308	40.3680	-160.78443120
-83.5769	40.2947	295.64080870
-83.5608	40.3414	522.59420953
-83.5647	40.3553	350.92933916
-83.5492	40.3669	362.56361978
-83.5278	40.3675	355.14619130
-83.5114	40.3642	319.81072259
-83.5161	40.3489	475.43037583
-83.5458	40.3444	381.26817756
-83.5769	40.2947	282.37120870
-83.5069	40.2947	459.37586444
-83.5100	40.2997	484.50371204
-83.5122	40.3022	473.60079658
-83.5144	40.3036	470.44132467
-83.5197	40.3178	440.13570666
-83.5294	40.3281	458.13876082
-83.5197	40.3333	417.14511927
-83.5769	40.2947	285.10680870
-83.5639	40.3008	280.12820621
-83.5883	40.2942	285.33861999
-83.6039	40.2856	291.81158032
-83.6086	40.2850	280.44037060

Appendix continued

Longitude	Latitude	Magnetic Residual (in gammas)
-83.6208	40.2878	303.14649726
-83.5967	40.2986	279.41137839
-83.6211	40.3108	335.52674741
-83.5769	40.2947	269.02140870
-83.7308	40.3680	-160.78863120
-83.7308	40.3680	-160.78443120
-83.5769	40.2947	286.01080870
-83.5964	40.2817	257.33671509
-83.5856	40.2875	240.42331010
-83.6014	40.2777	269.58804270
-83.6056	40.2692	276.50677079
-83.6125	40.2661	367.02178477
-83.5878	40.2633	358.97043311
-83.5903	40.2578	395.03593763
-83.5769	40.2947	255.21615028
-83.5847	40.2586	340.13283347
-83.5808	40.2550	415.30474180
-83.5564	40.2656	361.90746285
-83.5481	40.2567	740.14211874
-83.5283	40.2517	894.61980249
-83.5319	40.2592	970.95302059
-83.5419	40.2719	528.81084898
-83.5578	40.2689	305.55944032
-83.5769	40.2947	279.99115028
-83.5642	40.2758	257.07887501
-83.5489	40.2836	342.46078167
-83.5069	40.2744	711.88656816
-83.5769	40.2947	293.78015028
-83.7308	40.3680	-160.76143120
-83.7308	40.3680	-160.78443120
-83.8083	40.1944	-128.66774744
-83.8606	40.1981	-81.61115398
-83.8669	40.1994	-123.75692852
-83.8664	40.2022	-176.51039022
-83.8656	40.2136	-107.54587721
-83.8642	40.2281	-12.61145838
-83.8633	40.2342	-4.60417001
-83.8433	40.2336	16.46561407
-83.8444	40.2264	50.52173013
-83.8361	40.2183	-43.44867009
-83.8083	40.1944	-143.64274744
-83.8169	40.2175	-104.23985010
-83.8156	40.2317	17.51996829
-83.8139	40.2458	23.38636121
-83.8322	40.2489	10.39712272
-83.8039	40.2461	14.27914917
-83.7947	40.2467	74.72153234
-83.7847	40.2483	113.21859551
-83.7758	40.2467	-62.28662706
-83.8083	40.1944	-149.72234744
-83.7778	40.2219	22.24334038
-83.7614	40.2217	111.78229554
-83.7544	40.2483	72.26477171
-83.7506	40.2358	129.73372941
-83.7975	40.2239	58.65558523
-83.8083	40.1944	-185.72074744
-83.7308	40.3680	-160.80403120
-83.7308	40.3680	-160.78443120
-83.8083	40.1944	-191.54574744
-83.7969	40.2306	26.97561332

Appendix continued

Longitude	Latitude	Magnetic Residual (in gammas)
-83.7981	40.2164	60.23398033
-83.8083	40.2167	-0.03085206
-83.8183	40.2106	-1.47564228
-83.8375	40.2111	-28.78987731
-83.8378	40.2050	-48.26908620
-83.8392	40.1914	-82.57299407
-83.8203	40.1889	-116.82335468
-83.8133	40.1886	-15.30972093
-83.8083	40.1944	-109.64014744
-83.7806	40.1944	80.08700836
-83.7794	40.2017	34.68031309
-83.7619	40.1917	152.48056809
-83.7622	40.1847	120.71664824
-83.7639	40.1711	212.49941709
-83.7822	40.1722	112.29554658
-83.7847	40.1578	124.73282003
-83.7994	40.1586	109.95667967
-83.8083	40.1944	-160.58174744
-83.8133	40.1736	-3.88550593
-83.8317	40.1747	-196.71679476
-83.8411	40.1753	-120.36492644
-83.8592	40.1767	17.93821934
-83.8608	40.1692	36.16212999
-83.8619	40.1567	-50.25576646
-83.8733	40.1342	-210.18697956
-83.8083	40.1944	-106.91134744
-83.7308	40.3680	-160.79883120
-83.7308	40.3680	-160.78443120
-83.8083	40.1944	-158.24324744
-83.8431	40.1569	-18.38482914
-83.8531	40.1494	-53.89286164
-83.8547	40.1328	-15.61986542
-83.8369	40.1314	39.85933013
-83.8108	40.1294	190.47738256
-83.7792	40.1281	132.82423162
-83.7828	40.1447	87.90859584
-83.8083	40.1944	-178.52964744
-83.8131	40.1586	109.05717987
-83.8147	40.1564	43.81376393
-83.8161	40.1406	91.41900405
-83.8333	40.1550	-70.86549320
-83.8350	40.1461	-5.04881023
-83.8083	40.1944	-117.28734744
-83.6928	40.1847	347.02148168
-83.7064	40.2233	238.26618747
-83.7100	40.2189	203.36581152
-83.7292	40.2203	193.26999116
-83.7281	40.2356	183.80376105
-83.7286	40.2453	168.84187856
-83.7078	40.2289	262.24738032
-83.6953	40.2314	255.60695653
-83.6958	40.1878	286.44011063
-83.6928	40.1847	347.73508168
-83.7308	40.3680	-160.80543120
-83.7308	40.3680	-160.78443120
-83.6928	40.1847	339.73988168
-83.7114	40.2403	217.51557236
-83.7003	40.2425	174.76010130
-83.6953	40.2433	347.64914687
-83.6892	40.2439	240.99334972

Appendix continued

Longitude	Latitude	Magnetic Residual (in gammas)
-83.6650	40.2494	238.01804408
-83.6689	40.2372	305.81617394
-83.6650	40.2361	324.41177977
-83.6611	40.2236	218.75512287
-83.6592	40.2203	273.61007116
-83.6928	40.1847	312.63548168
-83.6819	40.2150	228.71314240
-83.6569	40.2125	452.10269490
-83.6494	40.2081	610.28280082
-83.6342	40.2094	842.04628728
-83.6442	40.2322	319.86043858
-83.6439	40.2361	435.34053209
-83.6281	40.2461	478.49111529
-83.6500	40.2397	436.49761204
-83.6928	40.1847	318.23918168
-83.7022	40.1878	216.31134503
-83.7106	40.2042	126.54476579
-83.7392	40.2058	227.07239501
-83.7092	40.2111	210.72389089
-83.7014	40.2108	188.77897121
-83.6911	40.2119	214.55999218
-83.6694	40.2092	268.64874559
-83.6928	40.1847	336.80488168
-83.7308	40.3680	-160.82413120
-83.7308	40.3680	-160.78443120
-83.6928	40.1847	340.01298168
-83.6850	40.2347	269.18272704
-83.6672	40.2031	405.14760462
-83.6625	40.1994	568.81262908
-83.6511	40.1925	830.19656810
-83.6708	40.1844	561.50258756
-83.6789	40.1831	420.39833282
-83.6811	40.1869	340.52405718
-83.6750	40.1931	430.32375342
-83.6928	40.1847	306.95038168
-83.7114	40.1889	106.05854592
-83.7194	40.1917	24.88176309
-83.7411	40.1939	198.76541375
-83.7419	40.1914	179.73900013
-83.7425	40.1842	211.56264319
-83.7425	40.1697	202.00538704
-83.7342	40.1689	219.27789472
-83.7142	40.1722	236.83455274
-83.6911	40.1803	302.13056856
-83.6928	40.1847	312.28778168
-83.6372	40.1814	1180.25852393
-83.6267	40.1775	1355.05882070
-83.6314	40.1681	1306.87288114
-83.6472	40.1739	1138.91458772
-83.6681	40.1653	668.71682556
-83.6850	40.1606	541.09494592
-83.6928	40.1847	338.79958168
-83.7308	40.3680	-160.78443120
-83.7308	40.3680	-160.78443120
-83.6928	40.1847	341.38068168
-83.7258	40.1544	244.71711588
-83.7361	40.1542	235.69023879
-83.7461	40.1556	191.45040445
-83.7369	40.1431	113.29304082
-83.7289	40.1308	158.98936621

Appendix continued

Longitude	Latitude	Magnetic Residual (in gammas)
-83.6947	40.1458	356.20105801
-83.6972	40.1550	345.70503620
-83.6928	40.1847	339.15538168
-83.6822	40.1542	561.32656939
-83.6711	40.1558	677.17770241
-83.6470	40.1522	1094.10092738
-83.6336	40.1525	1369.57975310
-83.6361	40.1419	1398.55603218
-83.6308	40.1414	1464.13242953
-83.6328	40.1267	1163.57148449
-83.6456	40.1392	1141.64274079
-83.6494	40.1400	1040.75667240
-83.6928	40.1847	343.95638168
-83.6778	40.1356	548.32921725
-83.6744	40.1278	597.88658286
-83.6800	40.1456	571.70583092
-83.7089	40.1419	346.62686098
-83.6928	40.1847	352.08928168
-83.7308	40.3680	-160.79033120
-83.7308	40.3680	-160.78443120
-83.5675	40.1911	1137.30538648
-83.6106	40.1975	1123.44045010
-83.6147	40.2125	1086.78253370
-83.6186	40.2206	874.79839152
-83.6128	40.2392	549.92275199
-83.5925	40.2489	501.25463023
-83.5897	40.2375	649.81215870
-83.5781	40.2233	945.49815691
-83.5864	40.2217	1027.14671509
-83.5675	40.1911	1121.07712269
-83.5747	40.2128	1055.27664166
-83.5461	40.2383	710.34746991
-83.5600	40.2319	813.93403158
-83.5703	40.2417	651.02804449
-83.5353	40.2481	764.10710222
-83.5236	40.2281	780.80741402
-83.5153	40.2303	939.55705176
-83.5211	40.2417	890.01756129
-83.5675	40.1911	1130.06862269
-83.5239	40.2469	894.81014598
-83.5036	40.2497	879.94042764
-83.5286	40.2197	852.60100764
-83.5389	40.2094	945.35447348
-83.5675	40.1911	1133.11408977
-83.7308	40.3680	-160.76963120
-83.7308	40.3680	-160.78443120
-83.5675	40.1911	1128.03052269
-83.5572	40.2194	932.19493528
-83.5342	40.2025	967.61799070
-83.5175	40.1889	1089.21527315
-83.5078	40.2014	1009.89291153
-83.5294	40.1431	1378.92144582
-83.5064	40.1514	1181.61355713
-83.5050	40.1706	1213.21575592
-83.5283	40.1558	1340.46735361
-83.5675	40.1911	1148.16032269
-83.5572	40.1917	1218.53348189
-83.5461	40.1800	1481.42235060
-83.5606	40.1739	1484.17854783
-83.5600	40.1633	1646.71027431

Appendix continued

Longitude	Latitude	Magnetic Residual (in gammas)
-83.6083	40.1664	1472.82301953
-83.6139	40.1761	1342.25147917
-83.5978	40.1711	1288.65686649
-83.5850	40.1792	1249.80365319
-83.5814	40.1814	1220.62827713
-83.5956	40.2011	1175.30198237
-83.5675	40.1911	1120.00258977
-83.5911	40.1572	1671.96369514
-83.6142	40.1664	1457.39158093
-83.5675	40.1911	1129.71298977
-83.7308	40.3680	-160.77253120
-83.7308	40.3680	-160.78443120
-83.5675	40.1911	1141.79678977
-83.6153	40.1550	1589.30217880
-83.6000	40.1292	1563.77699319
-83.5778	40.1317	1646.94304949
-83.5675	40.1911	1141.58792269